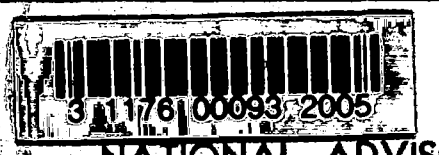

NATIONAL ADVISORY COMMITTEE FOR AERONAUTICS

WARTIME REPORT

ORIGINALLY ISSUED
April 1946 as
Advance Confidential Report L6C13

FIELD OF FLOW ABOUT A JET AND EFFECT OF JETS ON STABILITY OF JET-PROPELLED AIRPLANES

By Herbert S. Ribner

Langley Memorial Aeronautical Laboratory
Langley Field, Va.

NACA

WASHINGTON

NACA ACR No. L6C13

NATIONAL ADVISORY COMMITTEE FOR AERONAUTICS

ADVANCE CONFIDENTIAL REPORT

FIELD OF FLOW ABOUT A JET AND EFFECT OF JETS ON STABILITY OF JET-PROPELLED AIRPLANES

By Herbert S. Ribner

SUMMARY

The flow inclination induced outside cold and hot propulsive jets by the turbulent spreading has been derived. Certain simplifying assumptions were employed and the region near the orifice was not treated. The effect of jet temperature on the flow inclination was found to be small when the thrust coefficient is used as the criterion for similitude. The deflection of a jet due to angle of attack has been derived and found to be appreciable but small for normal flight conditions with small normal accelerations. The average jet-induced downwash over a tail plane has been obtained in terms of the geometry of the jet-tail configuration. These results have been applied to the estimation of the effect of the jets on the static longitudinal stability and trim of jet-propelled airplanes.

INTRODUCTION

A jet, as it spreads by turbulent mixing, is known to entrain outside air in the mixing zone. Air is thus drawn into the jet and the external flow is caused to incline toward the jet axis. If the jet passes near the tail surfaces of jet-propelled airplanes, the jet-induced flow deviation will affect the stability and trim. This flow deviation and its effects on static longitudinal stability are herein investigated theoretically for both cold and hot jets.

The present investigation was well advanced when a British report by Squire and Trouncer on the cold jet (reference 1) became available in this country. The considerable rigor of the British analysis was found to

be impaired by the use of an idealized cosine velocity distribution in the jet, which produces errors as great as 11 percent. Also, the original version of the present analysis was found to be oversimplified in one respect, which resulted in comparable errors in the opposite direction. In the present revised treatment, most of the advantages of simplification are retained, but the basic analysis of reference 1 is used to establish the value of a constant. The approximate treatment given herein permits the representation of the jet-induced stream deviation by a single curve. A comparison of the present analysis for the cold jet with that of Squire and Trouncer is given in appendix A. Reference 1 does not treat the hot jet.

The first part of the present paper is concerned with the analysis of the flow inclination induced outside cold and hot jets and the jet deflection due to angle of attack. The last part is concerned with applications to the computation of the effects of the jet on longitudinal stability and trim. The computational procedure is outlined in detail in the numerical example (tables I to III) so that little reference to the text is necessary.

SYMBOLS

(For diagrammatic representation of some of the symbols referring to jets, see fig. 1.)

F thrust

T absolute stream temperature, degrees

ρ stream density

σ ratio of local jet density to stream density

V stream velocity

u increment of jet velocity over stream velocity at point (x,r)

U increment of jet velocity over stream velocity at point x on jet axis

[redacted]

t increment of jet temperature over stream temperature at point (x,r), degrees

t_m increment of jet temperature over stream temperature at point x on jet axis

τ jet-temperature coefficient $\left(\frac{t/T}{u/V}\right)$

x axial distance from point at which jet, in accordance with law of spreading that holds at substantial distances from orifice, would have zero cross section

r radial distance from jet axis

R radius of jet boundary at section x

$$\eta = R\sqrt{\frac{\pi\rho V^2 I_1^2/2I_2}{F}} = R\sqrt{\frac{\pi I_1^2/I_2}{ST_c'}}$$

$$\xi = x\sqrt{\frac{\pi\rho V^2 I_1^2/2I_2}{F}} = x\sqrt{\frac{\pi I_1^2/I_2}{ST_c'}}$$

T_c' thrust coefficient $\left(\frac{F}{\frac{1}{2}\rho V^2 S}\right)$

S wing area

I_1, I_2 constants of velocity profile; defined in text

I_1', I_1'', I_2', and so forth functions of τ and U/V; defined in text

k jet-spreading parameter (taken as 0.240)

f jet-spreading parameter (taken as 3.3)

κ constant (taken as 0.31)

ψ stream function

[redacted]

ϵ jet-induced inclination of flow toward jet axis; with subscript w, wing downwash averaged between jet orifice and horizontal tail

$\bar{\epsilon}$ mean jet-induced downwash angle over horizontal tail

θ local inclination of jet axis to general flow

α angle of attack of thrust axis

α_e angle of attack of thrust axis relative to average flow between jet and tail $\left(\alpha - \epsilon_w\right)$

A area of jet orifice

b_t span of horizontal tail

d lateral distance of jet axis from center of horizontal tail

z distance of thrust axis below center of gravity

C_m airplane pitching-moment coefficient $\left(\frac{\text{Pitching moment}}{\frac{1}{2}\rho V^2 Sc}\right)$

c wing chord

l distance of nacelle inlet ahead of center of gravity; measured parallel to thrust axis

C_L airplane lift coefficient $\left(\frac{\text{Lift}}{\frac{1}{2}\rho V^2 S}\right)$; power on unless subscripted

i_t incidence of horizontal tail, degrees

δ_e elevator angle, degrees; positive downward

C_h elevator hinge-moment coefficient

$$\left(\frac{\text{Hinge moment}}{\frac{1}{2}\rho V^2 \times \text{Elevator span} \times (\text{Elevator chord})^2}\right)$$

[redacted]

$C_{h_\alpha} = \frac{dC_h}{d\alpha}$

$C_{h_\delta} = \frac{dC_h}{d\delta_e}$

n_p distance of neutral point behind leading-edge mean aerodynamic chord as fraction of mean aerodynamic chord

Δn_p shift of neutral point due to power; positive in forward direction

Subscripts:

j measured at jet orifice

T due to thrust force

ϵ due to jet-induced flow inclination

1 due to single jet

2 due to two jets

nac due to nacelle normal force

0 measured at zero thrust; defined as power-off condition

fixed stick fixed

free stick free

ASSUMPTIONS

The basic assumptions for the cold jet are the same as those for Prandtl's approximate treatment of the spread of turbulence (reference 2, pp. 163-165). The flow studied is incompressible but the results are considered closely applicable to all subsonic jets and approximately applicable to supersonic jets. The starting point for the present paper is a corollary of

[redacted]

the assumptions of reference 2, derived in appendix B in the form of an approximate differential equation for the spreading of a jet in a moving fluid. In reference 1 the spreading of the jet is obtained in a rigorous manner from first principles. It is shown in appendix B that by a suitable choice of a constant f the values of the two expressions can be made to agree very closely. The constant has been so chosen in the present analysis.

On the basis of experimental data (references 3 and 4) for a jet in still air, exclusive of the orifice region, the velocity profile is assumed to have the same shape at all sections of the jet. Thus no special consideration is given the region - approximately 8 orifice diameters in length - in which transition occurs from the uniform velocity at the jet orifice to the characteristic profile of the fully developed turbulent jet. The foregoing assumption is suitable for determining the downwash induced at the horizontal tail by wing-mounted jet motors; it is not suitable for determining the flow conditions near the jet orifice. The experimental velocity profile of reference 3 is used.

Velocity components parallel to the jet axis induced by the jet in the external flow are omitted in the analysis. This omission effects a considerable simplification in that it permits representation of the field of flow outside the jet by a single curve in a graph. As is pointed out in reference 1, neglect of the induced axial flow implies that "... the radial flow at each section of the jet [is] independent of the flow in other sections: this is approximately true very close to the boundary of the mixing region but is quite invalid at large distances from the jet axis. The actual flow outside the jet can be regarded as closely equivalent to that produced by a system of sinks along the jet axis, of strength sufficient to secure the proper inflow at the edge of the jet...." The results computed with this approximation are therefore restricted in applicability to the general vicinity of the jet. The region is more precisely defined subsequently in the present paper.

For the hot jet the assumption of incompressibility is abandoned for flow inside the jet but is retained for flow outside the jet. The perfect-gas law is applied, with the temperature elevation at any point in the jet assumed to be proportional to the difference between the local jet velocity and the stream velocity. Such a

[redacted]

temperature distribution is known to follow from the momentum-transfer theory when the temperature differences are so small that density changes and heat transfer by radiation may be neglected. This principle will be applied herein without restriction to small temperature differences and without regard for the divergence from experiment. (See fig. 2.) Because of these simplifying assumptions the analysis of the hot jet can hardly be valid quantitatively. The analysis should be valid qualitatively to the extent of establishing whether the effect of temperature on the jet-induced flow inclination is large or small.

ANALYSIS

Cold Jet Parallel to Stream

Velocity in jet.- If all the fluid of the jet is taken locally from the stream, momentum considerations show that the thrust equals the mass flow per second through any element multiplied by the excess of the jet velocity over the stream velocity at the element integrated over the cross section of the jet; that is (see fig. 1(a) for notation),

$$F = \rho \int_0^R (V + u)u \, 2\pi r \, dr$$

$$= 2\pi R^2 \rho U\left(VI_1 + UI_2\right)$$

or

$$\left(\frac{U}{V}\right)^2 + \frac{I_1}{I_2}\frac{U}{V} - \frac{F}{2\pi\rho V^2 I_2 R^2} = 0 \qquad (1)$$

where

$$I_1 = \int_0^1 \frac{u}{U}\frac{r}{R}\frac{dr}{R}$$

[redacted]

$$I_2 = \int_0^1 \left(\frac{u}{U}\right)^2 \frac{r}{R} \frac{dr}{R}$$

If any of the fluid of the jet is not taken from the stream, the thrust F in equation (1) must be replaced by (F - Flight velocity × Added mass per second). The added mass per second contributed by the fuel is negligible for air-breathing jet motors. For rockets the added mass per second equals the thrust divided by the jet-nozzle velocity. Aspirator-type jets lie between the two categories.

Equation (1) may be solved for the ratio of the peak jet additional velocity U to the stream velocity V in the form

$$\frac{U}{V} = \frac{I_1}{2I_2}\left(\sqrt{1 + \eta^{-2}} - 1\right) \qquad (2)$$

where

$$\eta = R\sqrt{\frac{\pi\rho V^2 {I_1}^2/2I_2}{F}}$$

$$= R\sqrt{\frac{\pi {I_1}^2/I_2}{ST_c'}}$$

and is a nondimensional parameter.

Spreading of jet.- By extension of Prandtl's qualitative reasoning (see reference 2, pp. 163-165) it is shown in appendix B that

$$\frac{dR}{dx} = \frac{k}{1 + f\frac{V}{U}} \qquad (B2)$$

where k and f are constants that are determined in appendixes A and B, respectively. By use of equation (2), equation (B2) may be written

[redacted]

$$\frac{dR}{dx} = \frac{k}{1 + \left(\frac{2fI_2}{I_1}\right)\left(\eta^2 + \eta\sqrt{\eta^2 + 1}\right)}$$

When the new variable

$$\xi = x\sqrt{\frac{\pi\rho V^2 I_1^2/2I_2}{F}}$$

$$= x\sqrt{\frac{\pi I_1^2/I_2}{ST_c'}}$$

is introduced

$$\frac{d\eta}{d\xi} = \frac{dR}{dx} = \frac{k}{1 + \left(\frac{2fI_2}{I_1}\right)\left(\eta^2 + \eta\sqrt{\eta^2 + 1}\right)} \tag{3}$$

and upon integration

$$\eta + \left(\frac{2fI_2}{3I_1}\right)\left[\eta^3 + \left(\eta^2 + 1\right)^{3/2} - 1\right] = k\xi \tag{4}$$

Equation (4) provides the law of spreading for the jet since $R \sim \eta$ and $x \sim \xi$; the thrust F is contained in both η and ξ. Near the origin, where the jet additional velocity U is large in comparison with the stream velocity V, η is small in comparison with unity and equation (4) is approximately

$$\eta = k\xi$$

or

$$R = kx$$

[redacted]

Thus, near the origin of the jet, the spreading is approximately linear with the axial distance x. Far from the origin, where the jet additional velocity is small in comparison with the stream velocity, η is large in comparison with unity and equation (4) is approximately

$$\frac{2fI_2}{3I_1} 2\eta^3 = k\xi$$

or

$$R^3 = \text{Constant} \times x$$

That is, far from the origin the jet spreads as the one-third power of the axial distance x. Some further comments on the spreading of a jet are made in appendix B.

For the velocity profile (fig. 2), experimentally found for a jet in a still fluid, $I_1 = 0.0991$ and $I_2 = 0.04895$. For greater generality k will be left undetermined for the present. With these values of I_1 and I_2, equation (4) has been used to prepare figure 3, which shows the variation of $R/\sqrt{ST_c'}$ with $kx/\sqrt{ST_c'}$. Equation (4) has also been used with equation (2) to provide the variation of U/V with $kx/\sqrt{ST_c'}$ shown in figure 4.

The point origin of the idealized jet of the present treatment, which is the origin of the coordinate x, is located a distance x_j upstream of the orifice of the actual jet. (See fig. 1.) The value of x_j varies with T_c' but an average value is 2.3 orifice diameters. More precise values can be obtained from figure 3 with R interpreted as the orifice radius R_j.

Flow inclination.- The condition of continuity may be expressed by forming the stream function

[redacted]

$$\psi = \int_0^r (u + V)r\, dr$$

Outside the jet this expression is approximately

$$\psi = UR^2 I_1 + \frac{Vr^2}{2} \tag{5}$$

if the small values of u induced by the jet in the external flow are ignored. The angle at which the external flow inclines toward the jet axis is then, for small angles,

$$\epsilon = \frac{1}{rV}\frac{\partial \psi}{\partial x}$$

$$= \frac{I_1}{r} R^2 \frac{dR}{dx}\left[2\frac{U/V}{R} + \frac{d(U/V)}{dR}\right] \tag{6}$$

The use of η and ξ in place of R and x, respectively, (with ratios of the form x/ξ permitted, however) serves to eliminate the thrust as a separate parameter. When this change is made in equation (6)

$$\epsilon = \frac{xI_1}{r\xi}\eta^2 \frac{d\eta}{d\xi}\left[\frac{2U/V}{\eta} + \frac{d(U/V)}{d\eta}\right]$$

if x/ξ is written for its equal R/η. Then by the use of equations (2) to (4) there results finally

$$\epsilon = \frac{kI_1^2}{2I_2}\frac{x}{r\xi}\frac{\left(\sqrt{\eta^2 + 1} - \eta\right)^2}{\left[1 + \left(\frac{2fI_2}{I_1}\right)\eta\left(\sqrt{\eta^2 + 1} + \eta\right)\right]\sqrt{\eta^2 + 1}} \tag{7}$$

in radians, where η is related to the independent variable ξ by equation (4). An asymptotic approximation, accurate to within 1 percent for $\eta \leq 0.18$, is

[redacted]

$$\epsilon = \frac{kI_1^2}{2I_2}\frac{x}{r\xi}\frac{1 - 2\eta}{1 + \left(2f\frac{I_2}{I_1}\right)\eta} \qquad (7a)$$

If η is expressed in terms of ξ^{-2}, the flow-inclination relation (7) is of the form

$$\epsilon = \text{Constant} \times \frac{x}{r} \times \text{Function of } \frac{ST_c'}{x^2}$$

Within the limits of application of equation (7) the flow inclination outside the jet thus is inversely proportional to the radial distance r from the jet axis. Equation (7) can be conveniently represented by the variation of $\frac{r}{x}\epsilon$ with $\frac{ST_c'}{x^2}$. The values of the constants k, f, I_1, and I_2 therein are determined in appendixes A and B as 0.240, 3.3, 0.0991, and 0.04895, respectively, for the velocity profile of figure 2. For these values the variation of $\frac{r}{x}\epsilon$ with $\frac{ST_c'}{x^2}$ is given in figure 5. This single curve provides all the necessary information on the flow inclination. A typical flow pattern is shown in figure 6.

The flow-inclination relation (7) and figure 5, which is computed from it, are limited in application to points reasonably near the jet but well away from the orifice. The first limitation results from the neglect in the computation of the stream function of values of axial velocity induced by the jet in the external flow. The second limitation results from the neglect of the transition region between the orifice of the jet and the region of similar velocity profiles. The charts of reference 1, in which these omissions were not made, show that the $\frac{1}{r}$-variation of equation (7) holds, in general, to ± 5 percent within twice the jet radius at distances greater than 8 orifice diameters downstream of the orifice. This accuracy should be sufficient for the usual relative positions of the jet and the horizontal tail for wing-mounted jet motors.

The foregoing remarks may be interpreted from another point of view. The diameter of the jet orifice does not appear in the equations of the flow analysis, but it has been ascertained that these equations are applicable, in general, for distances greater than 8 orifice diameters downstream of the orifice. The downwash induced at the horizontal tail by wing jets at a given thrust may therefore be concluded to be almost independent of the size of the jet orifice up to a diameter about one-eighth the distance to the horizontal tail.

For very high ratios of the jet velocity to the stream velocity $\left(\frac{U}{V} > 30\right)$, η is very small, and equations (7) and (7a) become approximately

$$\tan \epsilon = \frac{kI_1^2}{2I_2} \frac{x}{r\xi} = \frac{\sqrt{ST_c'}}{r}\left(\frac{kI_1}{\sqrt{4\pi I_2}}\right) \qquad (7b)$$

where the assumption that ϵ is small is dropped. Such conditions may occur with rockets at take-off and at low speeds. For rockets the mass flow from the nozzle is not taken from the stream and, as has been stated, the coefficient T_c' must be multiplied by one minus the ratio of the stream velocity to the jet exit velocity for use in the formulas. Rocket jets are ordinarily supersonic near the nozzle and the equations are not strictly applicable.

Hot Jet Parallel to Stream

Velocity in jet.- The local air density in the hot jet will be some variable fraction σ of the density in the free stream. For the present purpose the temperature elevation at any point in the jet will be assumed to be proportional to the difference between the local jet velocity and the stream velocity (see section of present paper entitled "Assumptions"); that is,

$$\frac{t}{T} = \frac{\tau u}{V}$$

[redacted]

where τ is a constant. (See fig. 1(b) for notation.) By the perfect-gas law then

$$\sigma = \frac{T}{T + t}$$

$$= \frac{1}{1 + \frac{t}{T}}$$

$$= \frac{1}{1 + \tau \frac{u}{U} \frac{U}{V}} \tag{3}$$

With the incorporation of the density factor σ, the equations for the cold jet will be modified to apply to the heated jet. The momentum equation will take the form

$$\left(\frac{U}{V}\right)^2 + \frac{I_1'}{I_2'} \frac{U}{V} - \frac{F}{2\pi\rho V^2 I_2' R^2} = 0 \tag{9}$$

where

$$I_1' = \int_0^1 \frac{\frac{u}{U} \frac{r}{R} \frac{dr}{R}}{1 + \tau \frac{u}{U} \frac{U}{V}}$$

$$I_2' = \int_0^1 \frac{\left(\frac{u}{U}\right)^2 \frac{r}{R} \frac{dr}{R}}{1 + \tau \frac{u}{U} \frac{U}{V}}$$

Comparison of I_1' and I_2' with the corresponding quantities for the cold jet, I_1 and I_2 (equation (1)), suggests the following approximations:

[redacted]

$$\left.\begin{aligned} \frac{I_1'}{I_2'} &= \frac{I_1}{I_2} \\ I_2' &= \frac{I_2}{1 + \frac{4I_2}{I_1} \kappa\tau \frac{U}{V}} \end{aligned}\right\} \qquad (10)$$

where κ is a constant to be determined by substituting values computed by the exact equations in the second of equations (10). An average value over the range of greatest interest, $0 \leqq \tau \frac{U}{V} \leqq 1.2$, is $\kappa = 0.31$ for the experimental velocity profile of figure 2. Equation (9) can now be expressed in the soluble form

$$\left(\frac{U}{V}\right)^2 + \frac{I_1}{I_2}\left(1 - \kappa\tau\eta^{-2}\right)\frac{U}{V} + \frac{I_1^2}{4I_2^2}\eta^{-2} = 0$$

from which

$$\frac{U}{V} = \frac{I_1/2I_2}{\eta^2 - \kappa\tau + \sqrt{\left(\eta^2 - \kappa\tau\right)^2 + \eta^2}} \qquad (11)$$

where η is the function of R and T_c' defined under equation (2).

The jet-temperature coefficient τ may be determined from the following considerations if the temperature at the jet orifice is known. Equation (9) as applied to conditions at the jet orifice (designated by subscript j), across which the velocity will be assumed uniform, takes the form

$$\left(\frac{U_j}{V}\right)^2 + \frac{U_j}{V} - \left(1 + \frac{t_j}{T}\right)\frac{T_c'S}{2A} = 0$$

[redacted]

whence

$$\frac{U_j}{V} = \frac{-1 + \sqrt{1 + 2\left(1 + \frac{t_j}{T}\right)\frac{T_c'S}{A}}}{2}$$

By application of its definition at the orifice, the temperature coefficient is

$$\tau = \frac{t_j/T}{U_j/V} \tag{12}$$

Spreading of jet.- It is shown in appendix B that

$$\frac{d\eta}{d\xi} = \frac{dR}{dx}$$

$$= \frac{k}{1 + \frac{fV}{U}} \tag{B2}$$

Substitution of equation (11) in equation (B2) gives

$$\left[1 + \frac{2fI_2}{I_1}\left(\eta^2 - \kappa\tau + \sqrt{\eta^4 + (1 - 2\kappa\tau)\eta^2 + \kappa^2\tau^2}\right)\right]\frac{d\eta}{d\xi} = k$$

The omission of η^4 in the radical considerably simplifies the integration and yields little error for $\eta^2 \ll 1$. With this omission the integral is

$$\eta + \frac{2fI_2}{I_1}\left[\frac{\eta^3}{3} - \kappa\tau\eta + \frac{\kappa\tau}{2a}\left(\eta\sqrt{\eta^2 + a^2} + a^2 \sinh^{-1}\frac{\eta}{a}\right)\right] = k\xi \tag{13}$$

[redacted]

where

$$a = \frac{\kappa\tau}{\sqrt{1 - 2\kappa\tau}}$$

Equation (13) provides the approximate law of spreading for the hot jet, since $R \sim \eta$ and $x \sim \xi$. The variation of $R/\sqrt{ST_c'}$ with $kx/\sqrt{ST_c'}$ for a typical hot jet ($\tau = 0.15$) is shown with the curve for the cold jet ($\tau = 0$) in figure 3. The variation of U/V with $kx/\sqrt{ST_c'}$ for $\tau = 0.15$, obtained by use of equation (13) with equation (11), is given in figure 4 along with the curve for the cold jet ($\tau = 0$).

Flow inclination.- The stream function for the hot jet is

$$\psi = \int_0^r \sigma(u + V)r\, dr$$

Outside the jet the expression is approximately

$$\psi = V\left[R^2\left(\frac{U}{V} I_1' - I_3'\right) + \frac{r^2}{2}\right]$$

where

$$I_3' = \int_0^1 (1 - \sigma)\frac{r}{R}\frac{dr}{R}$$

$$= \frac{1}{2} - \int_0^1 \frac{\frac{r}{R}\frac{dr}{R}}{1 + \tau\frac{u}{U}\frac{U}{V}} \qquad (14)$$

[redacted]

if the small values of u induced by the jet in the external flow are ignored. The jet-induced stream deviation is then, for small angles,

$$\epsilon = \frac{1}{Vr}\frac{\partial \psi}{\partial x}$$

$$= \frac{1}{r} R^2 \frac{dR}{dx}\left[2\frac{(U/V)I_1' - I_3'}{R} + \frac{U}{V}\frac{dI_1'}{dR} - \frac{dI_3'}{dR} + I_1'\frac{d(U/V)}{dR}\right]$$

The introduction of η and ξ in place of R and x, respectively, (with ratios of the form x/ξ permitted, however) eliminates the thrust as a separate parameter. With this change

$$\epsilon = \frac{x}{r\xi}\eta^2\frac{d\eta}{d\xi}\left[2\frac{(U/V)I_1' - I_3'}{\eta} + \frac{U}{V}\frac{dI_1'}{d\eta} - \frac{dI_3'}{d\eta} + I_1'\frac{d(U/V)}{d\eta}\right] \quad (15)$$

where x/ξ has been substituted for its equal R/η.

According to the original assumption that the shape of the velocity profile is the same for all sections, the ratio u/U depends only on r/R and is independent of R or η. Therefore

$$\left.\begin{aligned} \frac{dI_1'}{d\eta} &= \frac{d}{d\eta}\int_0^1 \frac{\frac{u}{U}\frac{r}{R}\frac{dr}{R}}{1 + \tau\frac{u}{U}\frac{U}{V}} = -I_1''\frac{d(U/V)}{d\eta} \\ \frac{dI_3'}{d\eta} &= \frac{d}{d\eta}\left(\frac{1}{2} - \int_0^1 \frac{\frac{r}{R}\frac{dr}{R}}{1 + \tau\frac{u}{U}\frac{U}{V}}\right) = I_3''\frac{d(U/V)}{d\eta} \end{aligned}\right\} \quad (16)$$

where

[redacted]

$$I_1'' = \tau \int_0^1 \frac{\left(\frac{u}{U}\right)^2 \frac{r}{R} \frac{dr}{R}}{\left(1 + \tau \frac{u}{U} \frac{U}{V}\right)^2}$$

$$I_3'' = \tau \int_0^1 \frac{\frac{u}{U} \frac{r}{R} \frac{dr}{R}}{\left(1 + \tau \frac{u}{U} \frac{U}{V}\right)^2}$$

Also, by differentiation of equation (11),

$$\frac{d(U/V)}{d\eta} = - \frac{I_1}{2I_2\eta^3} \left[2\kappa\tau - \frac{2\kappa\tau\left(\eta^2 - \kappa\tau\right) - \eta^2}{\sqrt{\left(\eta^2 - \kappa\tau\right)^2 + \eta^2}} \right] \tag{17}$$

The incorporation of equations (16) in equation (15) then yields the following final expression for the angle at which the flow inclines toward the axis of the hot jet:

$$\epsilon = \frac{x}{r\xi} \eta^2 \frac{d\eta}{d\xi} \left[2 \frac{(U/V)I_1' - I_3'}{\eta} - \left(\frac{U}{V} I_1'' + I_3'' - I_1' \right) \frac{d(U/V)}{d\eta} \right] \tag{18}$$

in radians. All of the variables in the equation except x and r are ultimately functions of η and τ alone; the I's and $d\eta/d\xi$ are given in terms of U/V and τ in equations (9), (14), (16), and (B2), and U/V, $d(U/V)/d\eta$, and ξ are given in terms of η and τ in equations (11), (17), and (13), respectively.

If η is expressed in terms of ξ^{-2} and τ by means of equation (13), the flow-inclination relation (18) is of the form

[redacted]

$$\epsilon = \text{Constant} \times \frac{x}{r} \times \text{Function of} \left(\frac{ST_c'}{x^2}; \tau \right)$$

As is the case for the cold jet, the flow inclination outside the jet is thus inversely proportional to the radial distance r. The effect of the jet temperature is determined by the jet-temperature coefficient τ.

Equation (18) for the flow deviation about the hot jet has been evaluated for the single value $\tau = 0.15$. The curve of $\frac{r}{x}\epsilon$ against $\frac{ST_c'}{x^2}$ is shown in figure 5, where ϵ is measured in degrees, along with the curve for the cold jet ($\tau = 0$).

Similitude of Hot and Cold Jets with Applications to Wind-Tunnel Tests

A typical value of the temperature coefficient in a propulsive jet is $\tau = 0.15$ at maximum flight T_c'. From the curves of figure 5, therefore, the effect of temperature on the jet-induced flow inclination can be seen to be small, provided the comparison is made at the same thrust coefficient T_c'. The thrust coefficient is thus a suitable criterion for the similitude of the flow fields about hot and cold jets of the type for which all the flow from the exit is supplied from the inlet. (For a constant throttle setting the coefficient τ increases as T_c' decreases, but this variation does not invalidate the conclusion.)

Because of the reduced density the hot jet from a typical thermal jet motor will have of the order of twice the exit velocity of a cold jet that develops the same thrust from the same size orifice, if all the flow from the exit is supplied from the inlet. The mass flow of the hot jet, however, will be of the order of one-half that of the cold jet. For model testing with a cold jet the mass flow into the nacelle inlet that would occur with a hot jet should be simulated in order to simulate the proper flow about the nacelle. The mass

[redacted]

flow in the cold jet can be made equal to that in the hot jet by reducing the orifice of the cold jet to such a size that the product of air density and orifice area is the same for both jets. In wind-tunnel tests at the Ames Aeronautical Laboratory of the NACA (unpublished) the scale-size orifice of the cold-jet model was restricted to an annulus by means of a faired plug.

If some of the fluid of the cold jet is supplied from a source other than the inlet of the nacelle, as in the case of an aspirator jet, the mass flow into the inlet is less than the mass flow from the exit, and the foregoing relations do not apply. In this case simulation of the proper mass flow into the inlet is possible without reduction of the size of the exit from the scale value. With an aspirator jet, however, the jet-induced flow inclination at a given thrust will be too small for the reasons explained in the analysis of the cold jet. (See section entitled "Cold Jet Parallel to Stream.")

Effect of Inclination of Jet Axis

General remarks.- The effect of inclination of the jet axis to the general flow must be considered in estimations of the jet-induced downwash at the tail plane. If the jet behaved like a rigid body the inclination would give rise to an interference similar to that between the fuselage and the horizontal tail. Vertically above the jet there would be a slight downwash, and on either side, a slight upwash. Averaged across the tail, the net effect would be negligible.

The jet actually approximates a rigid body in that it tends to maintain its shape and direction in spite of any inclination to the main flow. There is an appreciable progressive deviation, however, from the initial direction toward the stream direction that can be obtained from momentum considerations. This deflection alters the distance between the jet and the horizontal tail, and therefore the jet-induced downwash.

Determination of jet deflection.- Let θ be the local inclination of the jet axis to the general flow, and let α_e be the inclination of the thrust axis. On the basis of momentum considerations, the following approximate relation for the fractional angular deviation of the jet is derived in appendix C:

[redacted]

$$1 - \frac{\theta}{\alpha_e} = \frac{2 + \left(I_1 + 6K_T \frac{I_2}{I_1}\right)\frac{U}{V}}{2 + \left(2I_1 + 6K_T \frac{I_2}{I_1}\right)\frac{U}{V} + I_2\left(\frac{U}{V}\right)^2} \qquad (C3)$$

The variation of $1 - \frac{\theta}{\alpha_e}$ with $kx/\sqrt{ST_c'}$, for the cold jet ($T = 0$) and the hot jet ($T = 0.15$) is given in figure 7. The effect of jet temperature is seen to be negligible.

The change due to jet deflection in the radial distance r from the jet axis to the horizontal tail is given by

$$\Delta r = -\frac{\alpha_e}{57.3}(x - x_j)\left(1 - \frac{\theta}{\alpha_e}\right)_{av} \qquad (19)$$

where $x - x_j$ is the distance from the orifice to the horizontal tail and $\left(1 - \frac{\theta}{\alpha_e}\right)_{av}$ is the average value of $1 - \frac{\theta}{\alpha_e}$ between the jet orifice and the hinge line of the horizontal tail minus the value at the jet orifice. In this application the general flow in the region of the jet is affected by the wing downwash so that, in straight flight,

$$\alpha_e = \alpha - \epsilon_w$$

in degrees, where α is the inclination of the thrust axis to the free stream, and ϵ_w is the downwash due to the wing averaged over the length $x - x_j$. In accelerated flight the curvature of the flight path contributes an additional increment to α_e.

The jet deflection Δr is evaluated in table III of the numerical example, along with various other

[redacted]

quantities, and is shown to be no more than 15 percent of r. On the basis of these computations the jet deflection appears to be small for straight flight and for flight with small normal accelerations. On the other hand, the average angular deviation of the jet is an appreciable fraction of the angle of attack. The fractional angular deviation $\left(1 - \frac{\theta}{\alpha_e}\right)_{av}$ is 0.24 or greater for the several conditions of the numerical example. (See tables I to III.)

EFFECT OF JETS ON LONGITUDINAL STABILITY AND TRIM

Average Downwash over Tail Plane

Consider a general point y along the span of the horizontal tail, with y = 0 directly above the jet. (See fig. 8.) Let the angle subtended at the center of the jet by the length y be θ. The jet-induced flow inclination has been shown to be inversely proportional to the radial distance from the jet axis; therefore, if the inclination at y = 0 is ϵ, the inclination at y is $\epsilon \cos\theta$. The downwash at y is the component of this normal to the tail plane $\epsilon \cos^2\theta$. The unweighted mean downwash angle over the tail plane is therefore

$$\bar{\epsilon} = \frac{\int_{-d+\frac{b_t}{2}}^{d+\frac{b_t}{2}} \epsilon \cos^2\theta \, dy}{\int_{-d+\frac{b_t}{2}}^{d+\frac{b_t}{2}} dy}$$

$$= \frac{\epsilon r \int_{y=-d+\frac{b_t}{2}}^{y=d+\frac{b_t}{2}} d\theta}{b_t}$$

[redacted]

or

$$\frac{\bar{\epsilon}}{\epsilon} = \frac{r}{b_t}\left(\tan^{-1}\frac{-d+\frac{b_t}{2}}{r} + \tan^{-1}\frac{d+\frac{b_t}{2}}{r}\right) \qquad (20)$$

Lifting-line theory suggests that an average weighted according to the chord would provide the most accurate values of tail lift. An unweighted average over, say, 0.9 of the tail span would appear to approximate this condition. The curves of figure 8, accordingly, have been prepared from equation (20) with $0.9b_t$ substituted for b_t. The curves give the variation of $\bar{\epsilon}/\epsilon$ with r/b_t and $2d/b_t$ where $\bar{\epsilon}$ is now the effective mean jet-induced downwash across the tail plane, ϵ is the flow inclination at a radius r from the jet, and r/b_t and $2d/b_t$ locate the jet axis relative to the tail plane, as shown in figure 8. The curves apply to a single jet, and the downwash is additive for several jets.

Pitching-Moment Increments Due to Jet Operation

General considerations.- At a given angle of attack, operation of the jet motors will, in general, change both the pitching moment and the lift coefficient. Confusion will be avoided if the changes in pitching moment and lift coefficient are initially obtained as functions of the power-off (zero thrust) lift coefficient C_{L_O}, which is a known function of angle of attack. The several pitching-moment increments due to jet operation are discussed in the following paragraphs. Each increment is to be regarded as a function of C_{L_O}. The increments are given for a single jet and are to be multiplied by the number of jets.

Pitching moment contributed by direct thrust.- If the thrust axis of the jet passes a distance z below the center of gravity the thrust will contribute an incremental pitching moment, which is in coefficient form,

[redacted]

$$\Delta C_{m_T} = \frac{z}{c} T_c'$$

The thrust coefficient T_c' ordinarily will be known as a function of the power-on lift coefficient C_L. In order to obtain T_c' as a function of the power-off lift coefficient C_{L_0}, use can be made of the known relation between C_{L_0} and α together with the relation

$$C_L - C_{L_0} = \alpha T_c'$$

where C_L and C_{L_0} are measured at the same angle of attack α and α is taken in radian measure. A "cut-and-try" procedure may be used and a curve of C_L against C_{L_0} can be obtained at the same time.

Pitching moment contributed by jet-induced downwash.- It has been shown that a jet induces outside itself an axially symmetric flow field. The inclination ϵ (measured in degrees) relative to the thrust axis at the point (x,r) (see figs. 1 and 8) for a given thrust coefficient T_c', can be determined from figure 5. A small deflection Δr experienced by the jet when inclined to the general stream can be determined from equation (19) and figure 7 and used to correct r and then ϵ. The ratio of the value of average downwash over the horizontal tail $\bar{\epsilon}$ to the value of ϵ is given in figure 8 as a function of the geometry of the jet-tail configuration.

The pitching-moment coefficient contributed per jet by the jet-induced downwash is then, for the stick fixed,

$$\Delta C_{m_{\epsilon_{fixed}}} = - \frac{dC_m}{di_t} \bar{\epsilon}_1 \qquad (21)$$

If the stick is free and if the jet unit is mounted under the wing so that the horizontal tail is well away from the orifice, expression (21) becomes

[redacted]

$$\Delta C_{m_{\epsilon_{free}}} = -\left(\frac{dC_m}{di_t} - \frac{dC_m}{d\delta_e}\frac{C_{h_\alpha}}{C_{h_\delta}}\right)\bar{\epsilon}_1 \qquad (22)$$

If the orifice is near the horizontal tail, as when the jet issues from the rear end of the fuselage, the horizontal tail will be in a region of curved flow. If the value of C_{h_δ} is negative, the elevator will tend to float downward to conform to the curvature. This downfloating tendency will add a stabilizing or negative amount to the value of the stick-free pitching-moment increment given by equation (22). The change could be substantial for a closely balanced elevator (C_{h_δ} near zero); the magnitude of the change will depend on the type of balance. In addition, the hinge-moment characteristics might be modified by an effect of the jet on the boundary layer of the elevator.

The charts of the present paper (figs. 3, 4, 5, and 7) are not valid within a distance of approximately 8 orifice diameters downstream of the orifice, and reference 1 should be consulted for the flow in this region. Equation (21) for the stick-fixed pitching-moment increment will be approximately valid provided ϵ is evaluated at the three-quarter-chord line of the horizontal tail.

Pitching moment contributed by nacelle normal force.- The air taken in at the nacelle inlet is turned through an angle (the angle of attack of the thrust axis) in becoming alined with the jet axis. This turning of the air gives rise to a centrifugal force acting upward at the inlet. The force, which is negligible compared with the wing lift, equals the mass flow per second through the nacelle multiplied by the stream velocity and the sine of the local angle of attack. The contribution to the airplane pitching-moment coefficient is

$$\Delta C_{m_{nac}} = \frac{(\text{Mass/sec})\, l \sin(\alpha - \epsilon)}{\frac{1}{2}\rho V S c} \qquad (23)$$

[redacted]

where l is the lever arm from the inlet of the nacelle to the center of gravity of the airplane and $-\epsilon$ is the upwash induced by the wing at the nacelle inlet. The upwash $-\epsilon$ can be estimated from figure 5 of reference 5. This upwash is large only when l/c in equation (23) is small, and its neglect therefore introduces small error in the moment.

Pitching moment contributed by boundary-layer removal.- The suction and other effects of the jet may tend to remove some of the boundary layer on adjacent surfaces. The pressure distribution would be somewhat altered. In some instances flow separation may be inhibited, which would result in rather large changes in pressure distribution. In case flow separation on the wing is suppressed, an increased downwash will occur at the tail with a consequent positive pitching-moment increment. The determination of the moment changes due to these several effects must be left to experiment.

Any change in the fuselage pitching moment due to boundary-layer removal with tail on may possibly be different from such a change with tail off because of the interference between the horizontal tail and the fuselage. For this reason the comparison of tests of models with tail on and with tail off may not necessarily yield the part of the power-on pitching-moment change that can be attributed to the jet-induced downwash.

Neutral-Point Shifts Due to Power

The power-on curves of C_m against C_L for various elevator settings should be parallel like the power-off curves. The shift in neutral point due to power is therefore

$$\Delta n_p = \left(\frac{dC_m}{dC_L}\right)_{\text{Power on}} - \left(\frac{dC_m}{dC_L}\right)_{\text{Power off}}$$

in units of the wing chord. The derivatives are evaluated at any convenient elevator setting for the stick-fixed condition and at any convenient elevator tab setting for the stick-free condition.

[redacted]

From the earlier discussion it follows that expressions of the form

$$\Delta n_p = \frac{d\Delta C_m}{dC_{L_O}}$$

or

$$\Delta n_p = \frac{d\Delta C_m}{dC_L}$$

are not quite correct, where ΔC_m is the sum of the several incremental moment coefficients of the preceding paragraphs multiplied by the number of jet units, C_{L_O} is the power-off lift coefficient, and C_L is the power-on lift coefficient. Since $C_L - C_{L_O}$ is small, however, either of the two equations is a good first approximation. The exact neutral-point shift is slightly dependent on the position of the power-off neutral point.

Numerical Example and Discussion

Specifications for a hypothetical airplane propelled by twin wing-mounted jet motors are given in table I. Detailed computations of the effect of the jets on longitudinal stability and trim are given in tables II and III. Any moment resulting from boundary-layer removal that may be caused by jet action is not considered. The computations cover a range of lift coefficients and both cold and hot jets. The more important factors calculated are the mean jet-induced downwash angle over the horizontal tail; the changes in the pitching moment with the stick fixed and with the stick free due to this downwash, to the direct thrust moment, and to the nacelle normal force; and the corresponding shifts in the stick-fixed and stick-free neutral points.

Table II is a suggested short method of computation. The method is approximate in that the effect of jet deflection due to angle of attack is neglected, the variable distance x_j is taken as $4.6R_j$, and the effect

[redacted]

of temperature is neglected except in specifying the mass flow per second through the nacelle. Table III gives the detailed computation without these approximations. The maximum influence of the variation in x_j on the jet-induced flow inclination is found to be 1 percent. The maximum influence of both x_j and inclination of the jet axis on the mean jet-induced downwash is found to be 7 percent. The jet deflection does not exceed 15 percent of the distance from the jet axis to the horizontal tail. The close agreement between tables II and III suggests that the detailed computation of table III may be dispensed with in many cases.

Comparison with Experiment

The present method has been used to estimate the stick-fixed pitching-moment increments due to jet operation for a twin-jet fighter-type airplane that has been tested in the Langley full-scale tunnel. The unpublished experimental values are compared with the estimated values in figure 9. The flaps-neutral curves (fig. 9(a)) show a discrepancy in trim, but good agreement in slope. The flaps-deflected curves (fig. 9(b)) show good agreement in both slope and trim up to a lift coefficient of 0.6, but above $C_L = 0.6$ the experimental curve diverges markedly from the rather straight estimated curve. This divergence is probably associated with some suppression by jet action of separation at the nacelle inlets that was indicated by tuft studies carried out during the tests. On the whole, the agreement between the estimated pitching-moment increments due to jet operation and the experimental increments appears to be sufficient for design purposes. A number of further comparisons with experiment will have to be made before the accuracy of the method of estimation can be established.

CONCLUSIONS

An analysis has been made of the field of flow about a jet and the effect of jets on the stability and trim of jet-propelled airplanes. The following conclusions include an allowance for the limitations of the simplifying assumptions employed:

[redacted]

1. The jet-induced flow inclination varies very nearly inversely as the radial distance from the jet axis within the region between the jet boundary and twice the radius of the jet boundary at distances greater than 8 orifice diameters downstream of the orifice.

2. The effect of jet temperature on the jet-induced flow inclination is small when the thrust coefficient is used as the criterion for similitude.

3. The deflection of the jet due to angle of attack is small for straight flight and flight with small normal acceleration. The angular deviation of the jet, however, is an appreciable fraction of the angle of attack.

4. The downwash induced at the horizontal tail by wing jets at a given thrust is almost independent of the size of the jet orifice up to a diameter about one-eighth the distance to the horizontal tail.

5. The radius of a jet varies almost linearly with axial distance near the orifice and varies approximately as the one-third power of the axial distance very far from the orifice.

6. The equations for jet-induced flow inclination may be applied approximately to rocket jets if the thrust coefficient is multiplied by one minus the ratio of stream velocity to jet-nozzle velocity.

7. The influence of wing jets on longitudinal stability and trim may be estimated with sufficient accuracy for design purposes by an approximate method that neglects the effects of jet deflection, size of the jet orifice, jet-induced boundary-layer removal, and most of the effects of jet temperature.

Langley Memorial Aeronautical Laboratory
National Advisory Committee for Aeronautics
Langley Field, Va.

[redacted]

APPENDIX A

COMPARISON WITH THE ANALYSIS OF SQUIRE AND TROUNCER

The flow-inclination charts of Squire and Trouncer (reference 1) differ from figure 5 of the present paper by amounts from 0 to 11 percent when the flow is measured at the jet boundary 8 or more orifice diameters from the orifice. Figure 5 is believed to be more nearly correct within its region of application because of the use of an experimental rather than an idealized velocity distribution in the jet, although the treatment is less rigorous otherwise. A detailed comparison of the analyses follows.

Squire and Trouncer present a relatively rigorous treatment by the momentum-transfer theory of the development of a round jet in a general stream moving parallel to the jet axis. Full consideration is given to the region, approximately 8 orifice diameters in length, in which transition occurs from the uniform velocity at the jet orifice to the characteristic velocity distribution of the fully developed turbulent jet. The present analysis ignores the transition region entirely. Use is made of Squire and Trouncer's analysis to correct the value of a constant in an approximate equation for the spreading of the jet. (See appendix B.) The equation is derived from the qualitative considerations of reference 2.

In the analysis of reference 1 the values of axial velocity induced by the jet in the external flow are first neglected in determining the stream function, as has been done in the present analysis. Squire and Trouncer, however, use the result to determine a system of sinks along the jet axis from which the stream function (or, more accurately, its x-derivative) is reevaluated. This procedure effectively restores the missing axial-velocity increments. Examination of the computed flow-inclination charts of reference 1 in conjunction with the values of $\frac{1}{c^2 a U_1}\frac{\partial \psi}{\partial x}$ in tables II to IV therein shows that this refinement is unnecessary within twice the jet radius at points 8 or more orifice diameters downstream of the orifice. This range should cover the

[redacted]

usual relative positions of the jet and the horizontal tail for wing-mounted jet motors.

Determination of Jet-Spreading Parameter k

The only questionable point in the analysis of Squire and Trouncer is the use of a cosine-velocity distribution for reasons of mathematical simplicity, rather than the experimental velocity distribution that was used in the present analysis. The general development of the jet (from considerations of mass flow) is affected only slightly by a moderate change in the velocity profile. (See reference 1.) The determination of the angular spreading of the boundary of the jet by means of the experimental data of reference 1, however, is quite sensitive to the shape of the profile. The determination may be made as follows. A jet issuing from a small orifice in still air is known to spread conically. According to reference 1 the cone on which the velocity is equal to one-half the velocity on the jet axis at the same section has a semiangle of 5°. With Squire and Trouncer's cosine-velocity profile therefore

$$0.5R = x \tan 5^\circ$$

$$R = 0.175x$$

or

$$k = 0.175 \qquad (A1)$$

With the experimental velocity profile of reference 3 used herein (fig. 2),

$$0.365R = x \tan 5^\circ$$

$$R = 0.240x$$

$$k = 0.240 \qquad (A2)$$

This value is 37 percent more than the value for the cosine profile.

[redacted]

Effect of Velocity Profile on Flow Inclination

The flow inclination about the jet is in turn dependent on the spreading of the jet. If η is expressed in terms of ξ^{-2}, equation (7) is of the form

$$\frac{r}{x}\epsilon = \frac{k^2 I_1^2}{I_2} \times \text{Function of} \left[\frac{ST_c'}{x^2\left(\frac{k^2 I_1^2}{I_2}\right)} ; \frac{fI_2}{I_1} \right] \qquad (A3)$$

where k and f are parameters for the spreading of the jet, and I_1 and I_2 are integrals involving the velocity profile. With Squire and Trouncer's cosine profile

$$\frac{k^2 I_1^2}{I_2} = \frac{(0.175)^2(0.1486)^2}{0.0861}$$

$$= 0.00785$$

$$\frac{fI_2}{I_1} = \frac{(2.6)\ (0.0861)}{0.1486}$$

$$= 1.506$$

With the experimental velocity profile (fig. 2)

$$\frac{k^2 I_1^2}{I_2} = \frac{(0.240)^2(0.0991)^2}{0.04895}$$

$$= 0.01156$$

[redacted]

$$\frac{fI_2}{I_1} = \frac{(3.3)(0.04895)}{0.0991}$$

$$= 1.632$$

The difference in $k^2 I_1^2/I_2$ is 32 percent of the value for the experimental profile. This difference is large enough to reduce the ordinates of figure 5 by from 0 to 11 percent; the reduction is almost linear with ST_c'/x^2 up to a value of 7 percent at $\frac{ST_c'}{x^2} = 0.8$. With this reduction, figure 5 is in substantial agreement, within its range of applicability, with the charts of reference 1. The use of a cosine-velocity distribution instead of the more sharply peaked experimental distribution thus appears to introduce errors up to 11 percent in the charts of reference 1.

It is rather striking that the pronounced difference between the cosine profile and the experimental velocity profile results in very little difference in the parameter fI_2/I_1. Thus the only important uncertainty in the calculations for the cold jet is the evaluation of the spreading-profile parameter $k^2 I_1^2/I_2$. This uncertainty is not great, since 32 percent error in $k^2 I_1^2/I_2$ leads to errors of from 0 to 11 percent in the flow inclination.

These results imply that the calculated rate of change of mass flow in the jet with axial distance is not critically dependent on the velocity profile chosen. Presumably Squire and Trouncer had this interpretation in mind when they stated (reference 1) that the general development of the jet is little affected by a moderate change in velocity profile.

[redacted]

APPENDIX B

APPROXIMATE DIFFERENTIAL RELATION FOR SPREADING OF ROUND JET OR WAKE IN MOVING FLUID AND ESTABLISHMENT OF THE CONSTANT f FROM EQUATIONS (14) AND (15) OF SQUIRE AND TROUNCER

Basic Analysis

Consider a cross section of a round jet or wake for which the velocity at the center is U. The particles of fluid in the section move downstream with an average velocity $\frac{U}{2} + V$. According to Prandtl's approximate treatment of the spread of turbulence (reference 2, pp. 163 to 165) the time rate of increase of the jet radius is proportional to the velocity difference $|U|$ between the center of the jet and the edge. The section may thus be visualized as expanding radially with a velocity proportional to $|U|$ and moving downstream with a velocity $\frac{U}{2} + V$. The slope of the boundary of this round jet or wake is therefore

$$\frac{dR}{dx} \sim \frac{U}{\frac{U}{2} + V} = k \frac{U}{U + 2V} \tag{B1}$$

where k is a constant that is determined in appendix A from experimental data. Equation (B1) is also applicable to a two-dimensional jet or wake if R is interpreted as the semiwidth.

Equation (B1) leads to the known linear expansion of the jet radius with axial distance for a round jet in still air and to the known one-third power law for the wake of a body of revolution. The proofs, which are simple, are omitted. It is of interest to note that a high-speed jet in moving air should show an approximately linear spreading near the orifice, where the stream

[redacted]

velocity V is small in comparison with the jet additional velocity U, and far back where U is small in comparison with V the expansion should follow the one-third power law for the spreading of the wake of a body of revolution.

The foregoing analysis contains an arbitrary element in the specification of $\frac{U}{2} + V$ as the effective average velocity in the jet. A more generalized average velocity would be $\frac{U}{f} + V$ where f is a constant that depends on the shape of the velocity profile. Thus equation (B1) can be generalized to

$$\frac{dR}{dx} = k \frac{|U|}{U + fV} \tag{B2}$$

It will be shown that the equations of reference 1, derived on a more rigorous basis, provide an expression for dR/dx that approximates equation (B2) very closely for a suitable value of f, and thus establish the correct value for f.

Determination of Jet-Spreading Parameter f

Equations (14) and (15) of reference 1 may be written, in the notation of the present paper, as

$$UR^2\left(I_1 V + I_2 U\right) - b_3 = 0 \tag{B3}$$

$$U \frac{dR}{dx}\left(b_1 V + b_2 U\right) + R \frac{dU}{dx}\left(b_3 V + b_4 U\right) + b_5 U^2 = 0 \tag{B4}$$

respectively, where

[redacted]

$$I_1 = \int_0^1 \frac{u}{U}\frac{r}{R}\frac{dr}{R} = 0.1486 \qquad b_1 = 2\left(J_1 - \frac{1}{16}\right) = 0.0578$$

$$I_2 = \int_0^1 \left(\frac{u}{U}\right)^2 \frac{r}{R}\frac{dr}{R} = 0.0861 \qquad b_2 = 2\left(J_2 - \frac{1}{2}J_1\right) = 0.0476$$

$$J_1 = \int_0^{\frac{1}{2}} \frac{u}{U}\frac{r}{R}\frac{dr}{R} = 0.0914 \qquad b_3 = J_1 = 0.0914$$

$$J_2 = \int_0^{\frac{1}{2}} \left(\frac{u}{U}\right)^2 \frac{r}{R}\frac{dr}{R} = 0.0695 \qquad b_4 = 2J_2 - \frac{1}{2}J_1 = 0.0933$$

$$b_5 = \frac{\pi c^2}{8}$$

The numerical values apply to the cosine-velocity distribution adopted by Squire and Trouncer. (The symbol c in the equation for b_5 is used by Squire and Trouncer and is distinct from the wing chord c of the present report.) Elimination of dU/dx between equations (B3) and (B4) gives

$$\frac{dR}{dx} = \frac{-b_5 U\left(I_1 V + 2I_2 U\right)}{-\left(2I_1 V + 2I_2 U\right)\left(b_3 V + b_4 U\right) + \left(I_1 V + 2I_2 U\right)\left(b_1 V + b_2 U\right)} \tag{B5}$$

If this equation is put into the form of equation (B2), the constants therein are

$$k = \frac{\frac{\pi c^2}{8}}{b_4 - b_2}$$

[redacted]

$$f = f\left(\frac{V}{U}\right) = \frac{b_3 - b_1}{b_4 - b_2} + \frac{I_1\left(b_3 + b_4 \frac{U}{V}\right)}{\left(b_4 - b_2\right)\left(I_1 + 2I_2 \frac{U}{V}\right)} \qquad (B6)$$

For the values of the constants that apply to the cosine-velocity profile of Squire and Trouncer (given under equation (B4)), an average value for f is 2.6. With this value the approximate equation (B2) agrees with the more exact equation (B5) within 1 percent over the range from $\frac{U}{V} = 1$ to $\frac{U}{V} = \infty$.

For the experimental velocity profile that was used herein (fig. 2) the constants are

$I_1 = 0.0991$ $\qquad$ $b_1 = 0.01514$

$I_2 = 0.04895$ $\qquad$ $b_2 = 0.01764$

$J_1 = 0.0701$ $\qquad$ $b_3 = 0.0701$

$J_2 = 0.0439$ $\qquad$ $b_4 = 0.0527$

Insertion of these values in equation (B6) gives an average value of 3.3 for f. With this value the approximate equation (B2) agrees with the more exact equation (B5) within 2 percent over the range from $\frac{U}{V} = 1$ to $\frac{U}{V} = \infty$. The value $f = 3.3$ has been used in the computations of the present paper.

APPENDIX C

DEFLECTION OF IDEAL JET INCLINED TO STREAM

Let α_e be the inclination of the thrust axis to the general flow, and let θ be the inclination of the jet center line at a distance x from the fictitious point origin of the jet. It is required to determine $1 - \frac{\theta}{\alpha_e}$, the fractional change in the direction of the jet.

The momentum relations for the components of the thrust parallel to and perpendicular to the stream are, for small values of α_e,

$$T = \rho \int_0^R \sigma(V + u)u \, 2\pi r \, dr$$

$$= 2\pi R^2 \rho V^2 \left[\frac{U}{V} I_1' + \left(\frac{U}{V}\right)^2 I_2' \right] \qquad (C1)$$

$$\alpha_e T = \rho \int_0^R \sigma(V + u)^2 \theta \, 2\pi r \, dr + \rho \int_0^R V^2 \theta \, 2\pi r \, dr$$

The first integral of $\alpha_e T$ is the cross-wind momentum of the mass flow in the jet; the second integral is the cross-wind momentum of the disturbed outside air computed from the additional apparent mass of the jet. The expression reduces to

$$\alpha_e T = \theta \, 2\pi R^2 \, \rho V^2 \left[2 - I_3' + 2\frac{U}{V} I_1' + \left(\frac{U}{V}\right)^2 I_2' \right] \qquad (C2)$$

Solving equations (C1) and (C2) simultaneously gives

[redacted]

$$1 - \frac{\theta}{\alpha_e} = \frac{2 - I_3' + \frac{U}{V} I_1'}{2 - I_3' + \frac{U}{V} I_1' + \left(\frac{U}{V}\right)^2 I_2'}$$

In accordance with the main text put

$$I_1' \approx \frac{I_1}{1 + \frac{4I_2}{I_1} K_T \frac{U}{V}}$$

$$I_2' \approx \frac{I_2}{1 + \frac{4I_2}{I_1} K_T \frac{U}{V}}$$

$$I_3' \approx \frac{\frac{2I_2}{I_1} K_T \frac{U}{V}}{1 + \frac{4I_2}{I_1} K_T \frac{U}{V}}$$

(Strictly speaking, the values of K should be different in each expression.) Then

$$1 - \frac{\theta}{\alpha_e} = \frac{2 + \left(I_1 + 6K_T \frac{I_2}{I_1}\right)\frac{U}{V}}{2 + \left(2I_1 + 6K_T \frac{I_2}{I_1}\right)\frac{U}{V} + I_2\left(\frac{U}{V}\right)^2} \qquad (C3)$$

[redacted]

REFERENCES

1. Squire, H. B., and Trouncer, J.: Round Jets in a General Stream. R. & M. No. 1974, British A.R.C., 1944.

2. Prandtl, L.: The Mechanics of Viscous Fluids. Spread of Turbulence. Vol. III of Aerodynamic Theory, div. G, sec. 25, W. F. Durand, ed., Julius Springer (Berlin), 1935, pp. 162-175.

3. Fluid Motion Panel of the Aeronautical Research Committee and Others: Modern Developments in Fluid Dynamics. Vol. II, ch. XIII, sec. 255; S. Goldstein, ed., The Clarendon Press (Oxford), 1938, p. 596, fig. 236.

4. Corrsin, Stanley: Investigation of Flow in an Axially Symmetrical Heated Jet of Air. NACA ACR No. 3L23, 1943.

5. Ribner, Herbert S.: Notes on the Propeller and Slipstream in Relation to Stability. NACA ARR No. L4I12a, 1944.

[redacted]

TABLE I

SPECIFICATIONS FOR NUMERICAL EXAMPLE

Twin wing jets	
S, square feet	275
R_j, foot	0.4
r, feet	3
$x - x_j$ (to hinge line of horizontal tail), feet	8
d, feet	3
b_t, feet	12
l/c	0.5
z/c	0.1
dC_m/di_t	-0.030
$dC_m/d\delta_e$	-0.015
$C_{h_\alpha}/C_{h_\delta}$	0.5
T_c' per jet	$0.16C_{L_0}$
Jet temperature minus stream temperature t_j, °F	1430
Stream temperature T, °F abs	530

NATIONAL ADVISORY
COMMITTEE FOR AERONAUTICS

[redacted]

TABLE II

SHORT APPROXIMATE COMPUTATIONS FOR NUMERICAL EXAMPLE

[Jet deflection neglected and x_j taken as $4.6R_j$; jet temperature neglected except in step 13]

Step	Jet (assumed) / Flap deflection, deg / Parameter	Cold 0	Cold 0	Cold 45	Cold 45	Remarks Given
1	C_{L_0}	0.5	1.0	1.0	2.0	Given
2	T_c'	.08	.16	.16	.32	Given
3	ST_c'/x^2	.227	.455	.455	.909	$\frac{S}{x^2}$ × step 2
4	$\frac{r}{x}\epsilon$	.222	.420	.420	.750	From fig. 5, by use of step 3 (curve for $\tau = 0$)
5	ϵ, deg	.73	1.38	1.38	2.46	Jet-induced downwash angle at section of horizontal tail vertically above jet $\left(\text{step } 4 \times \frac{x}{r}\right)$
6	r/b_t	.25	.25	.25	.25	r and b_t given in table I
7	$2d/b_t$	.5	.5	.5	.5	d given in table I
8	$\bar{\epsilon}/\epsilon$	.526	.526	.526	.526	From fig. 8 by use of steps 6 and 7
9	$\bar{\epsilon}_2$, deg	.77	1.45	1.45	2.59	Mean jet-induced downwash angle over horizontal tail for two jets (2 × step 5 × step 8)
10	$\Delta C_{m_{\epsilon_{fixed_2}}}$	.0231	.0435	.0435	.0777	Pitching-moment increment due to jet-induced downwash; stick fixed $\left(-\frac{dC_m}{di_t} \times \text{step } 9\right)$
11	$\Delta C_{m_{\epsilon_{free_2}}}$	.0173	.0326	.0326	.0583	Pitching-moment increment due to jet-induced downwash; stick free $\left[-\left(\frac{dC_m}{di_t} - \frac{dC_m}{d\delta_e}\frac{C_{h_\alpha}}{C_{h_\delta}}\right) \times \text{step } 9\right]$
12	$\Delta C_{m_{T_2}}$	.0160	.0320	.0320	.0640	Pitching-moment increment due to thrust-axis offset $\left(2 \times \frac{z}{c} \times \text{step } 2;\ \frac{z}{c} \text{ from table I}\right)$
13	$\frac{\text{Mass/sec}}{\rho VS}$	.00470	.00654	.00654	.00914	Mass flow through nacelle at sea level; hot jet; in coefficient form (given)
14	α, deg	3.7	10.3	-.3	13.0	Given
15	$\Delta C_{m_{nac_2}}$	.0006	.0024	-.0001	.0042	Pitching-moment increment due to nacelle normal force, with wing upwash neglected $\left(4\frac{l}{c} \times \text{step } 13 \times \sin \text{step } 14\right)$
16	$\Delta n_{p_{fixed}}$	.078	.073	.073	.068	Stick-fixed neutral-point shift due to power [slope of curve of (step 10 + step 12 + step 15) against C_{L_0}]
17	$\Delta n_{p_{free}}$	.068	.064	.064	.061	Stick-free neutral-point shift due to power [slope of curve of (step 11 + step 12 + step 15) against C_{L_0}]

[redacted]

TABLE III

DETAILED COMPUTATIONS FOR NUMERICAL EXAMPLE

Step	Jet (given) / Flap deflection, deg / Parameter	Cold 0	Cold 0	Cold 45	Cold 45	Hot 45	Remarks Given
1	C_{L_0}	0.5	1.0	1.0	2.0	2.0	Given
2	T_c'	.08	.16	.16	.32	.32	Given
3	t_j/T	0	0	0	0	2.70	Given
4	U_j/V	4.15	6.13	6.13	8.87	17.5	Ratio of outlet velocity minus stream velocity to stream velocity (from equation (12))
5	τ	0	0	0	0	.159	Ratio of absolute temperature to velocity $\left(\frac{\text{step 3}}{\text{step 4}}\right)$
6	$R_j/\sqrt{ST_c'}$	.085	.060	.060	.043	.043	R_j and S given in table I; T_c' given in step 2
7	$kx_j/\sqrt{ST_c'}$	.096	.066	.066	.047	.043	From fig. 3 with step 6 used as abscissa
8	x_j, ft	1.88	1.83	1.83	1.84	1.68	Distance upstream from orifice of point origin of equivalent ideal jet
9	x, ft	9.88	9.83	9.83	9.84	9.68	Axial distance from origin of equivalent ideal jet to point under consideration; in this case, the hinge line of horizontal tail
10	ST_c'/x^2	.225	.455	.455	.909	.939	$ST_c'/(\text{step 9})^2$
11	$\frac{r}{x}\epsilon$	.220	.420	.420	.750	.722	From fig. 5, by use of steps 5 and 10
12	$kx/\sqrt{ST_c'}$	.506	.372	.372	.252	.248	$\left(0.240/\sqrt{ST_c'}\right) \times$ step 9
13	$\left(1 - \frac{\theta}{a_e}\right)_{av}$	.34	.31	.31	.24	.24	Average of curve of $1 - \frac{\theta}{a_e}$ between values of $kx/\sqrt{ST_c'}$ given by steps 7 and 12, respectively, minus value of $1 - \frac{\theta}{a_e}$ for step 7
14	a, deg	3.7	10.3	-.3	13.0	13.0	Given
15	ϵ_w, deg	2.5	5.1	10.0	15.1	15.1	Wing downwash, estimated
16	a_e, deg	1.2	5.2	-10.3	-2.1	-2.1	Average inclination of flow relative to the initial direction of the jet axis (step 14 - step 15)
17	Δr, ft	-.06	-.23	.45	.07	.07	Jet deflection at horizontal tail due to inclination to the stream $\left[-(x - x_j) \times \text{step 13} \times \frac{\text{step 16}}{57.3}\right]$
18	r, ft	2.94	2.77	3.45	3.07	3.07	Dimension r (fig. 7) corrected for jet deflection (3.00 + step 17)
19	ϵ, deg	.74	1.49	1.20	2.40	2.27	Jet-induced flow inclination at point of horizontal tail vertically above jet $\left(\text{step 9} \times \frac{\text{step 11}}{\text{step 18}}\right)$
20	r/b_t	.245	.231	.288	.256	.256	Step $18/b_t$
21	$2d/b_t$	.5	.5	.5	.5	.5	d and b_t given in table I
22	$\bar{\epsilon}/\epsilon$	.522	.502	.570	.533	.533	From fig. 8 with the use of steps 20 and 21
23	$\bar{\epsilon}_2$, deg	.77	1.55	1.37	2.56	2.42	Mean jet-induced downwash over horizontal tail, for two jets (2 x step 19 x step 22)
		.77	1.45	1.45	2.59	------	Approximate value from table II for comparison
From this point the procedure of table II is followed.							

[redacted]

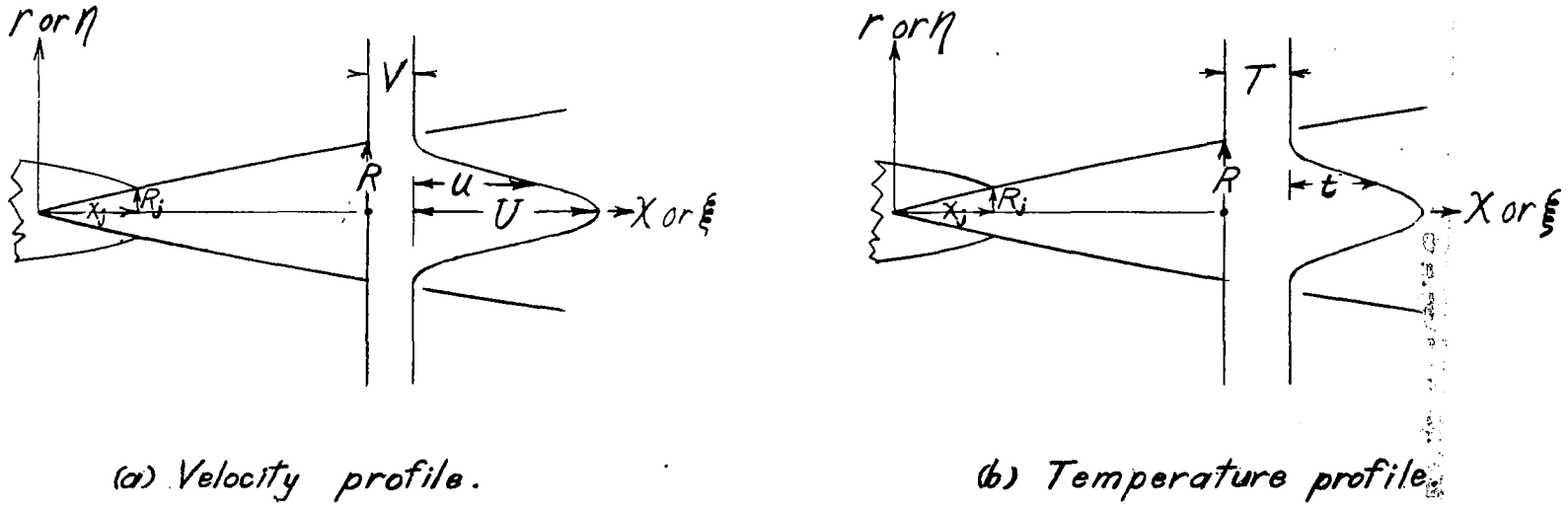

(a) Velocity profile.

(b) Temperature profile.

NATIONAL ADVISORY
COMMITTEE FOR AERONAUTICS

Figure 1.- Notation for the velocity and temperature profiles in the jet. The base line for the temperature profile is absolute zero. See also section entitled "Symbols."

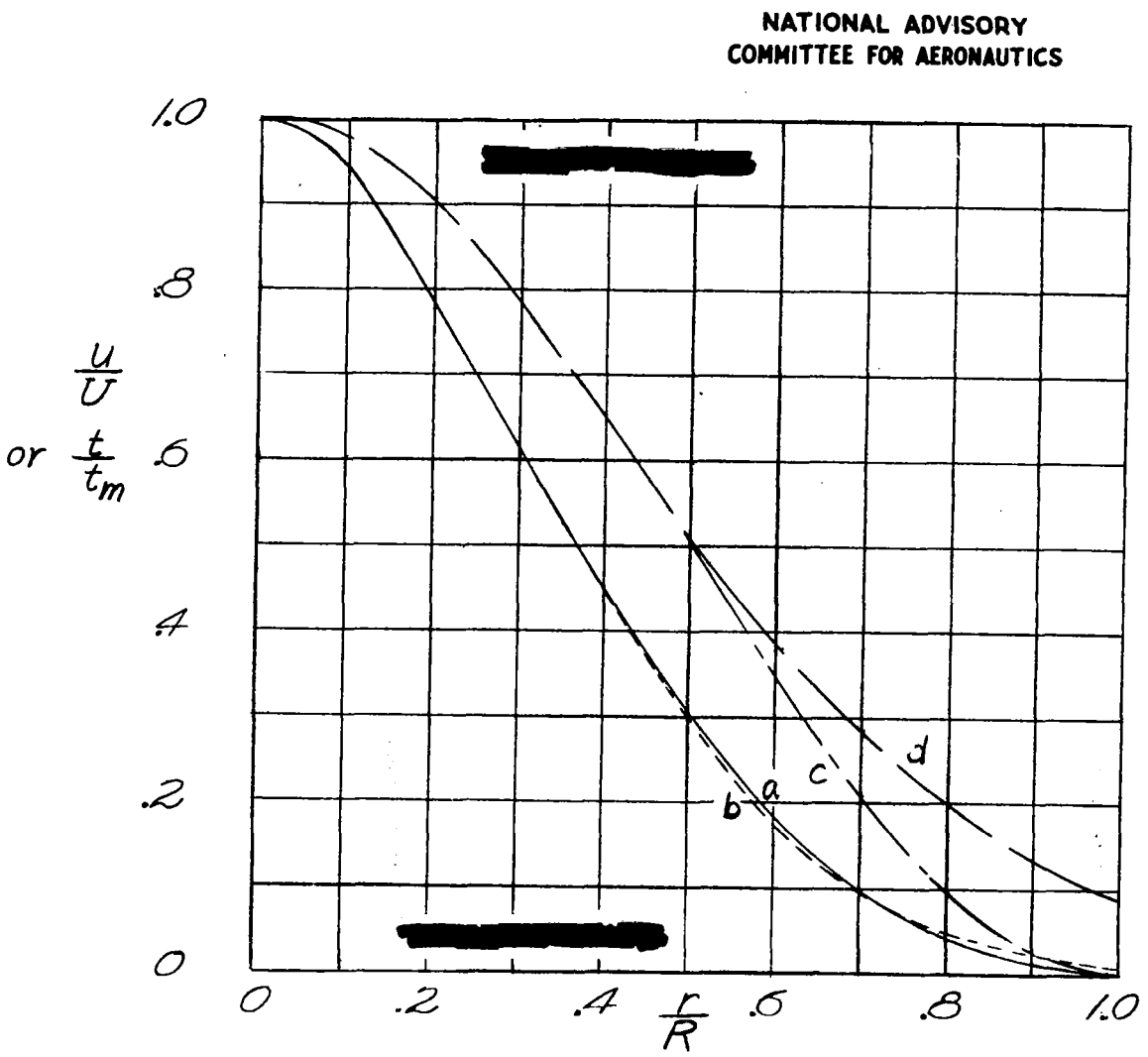

Figure 2.- Velocity and temperature profiles for a round jet in still air.

(a) Experimental velocity profile adopted for the present report. Replotted from reference 3 with r/R taken as the value therein divided by 2.74.

(b) Experimental velocity profile of figure 20 of reference 4 fitted to curve (a) at $\frac{u}{U} = 0.5$.

(c) Theoretical cosine velocity profile of reference 1.

(d) Experimental temperature profile of figure 20 of reference 4 to same r/R scale as curve (b).

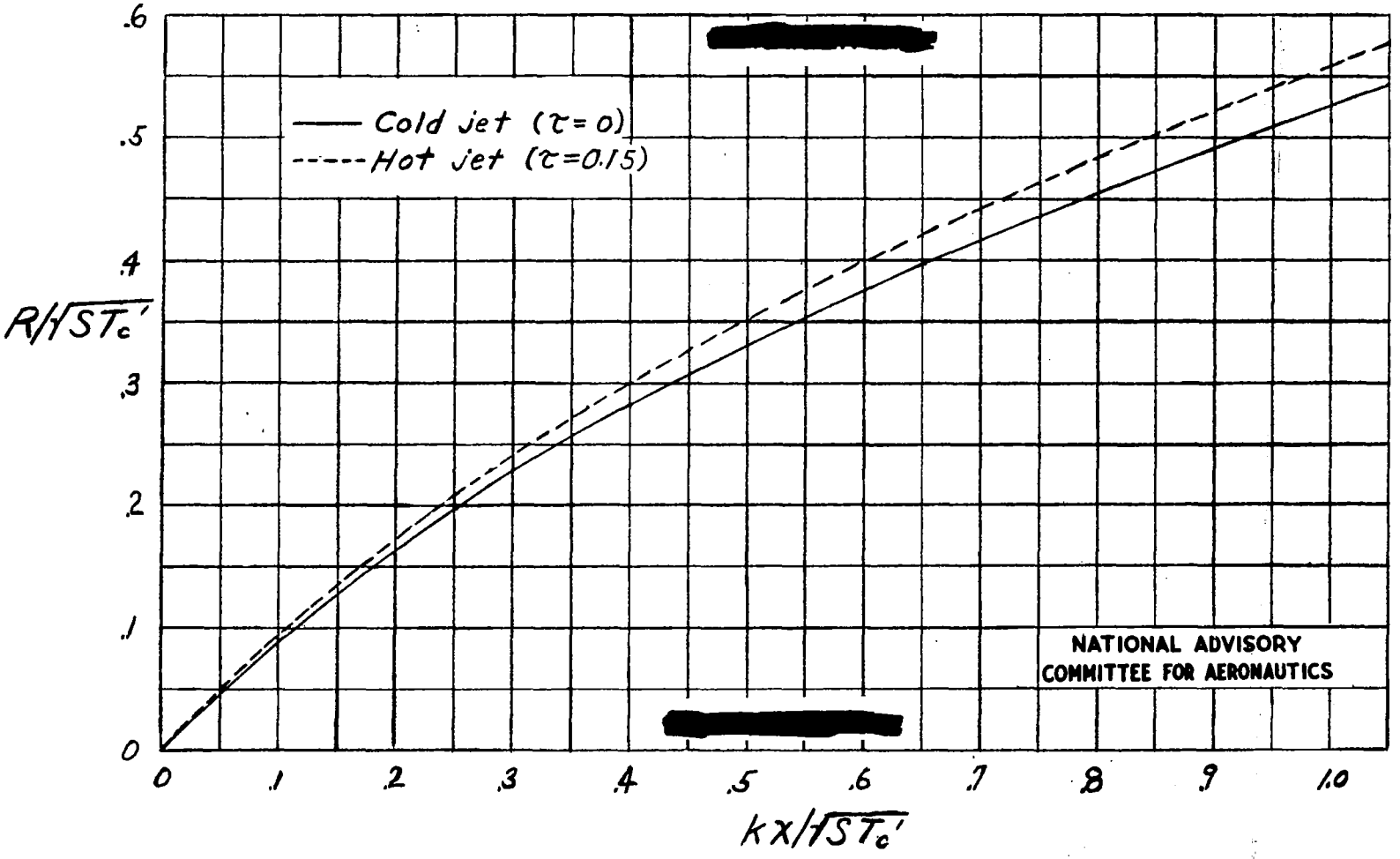

Figure 3.- Spreading of the jet: variation of $R/\sqrt{ST_c'}$ with $kx/\sqrt{ST_c'}$.

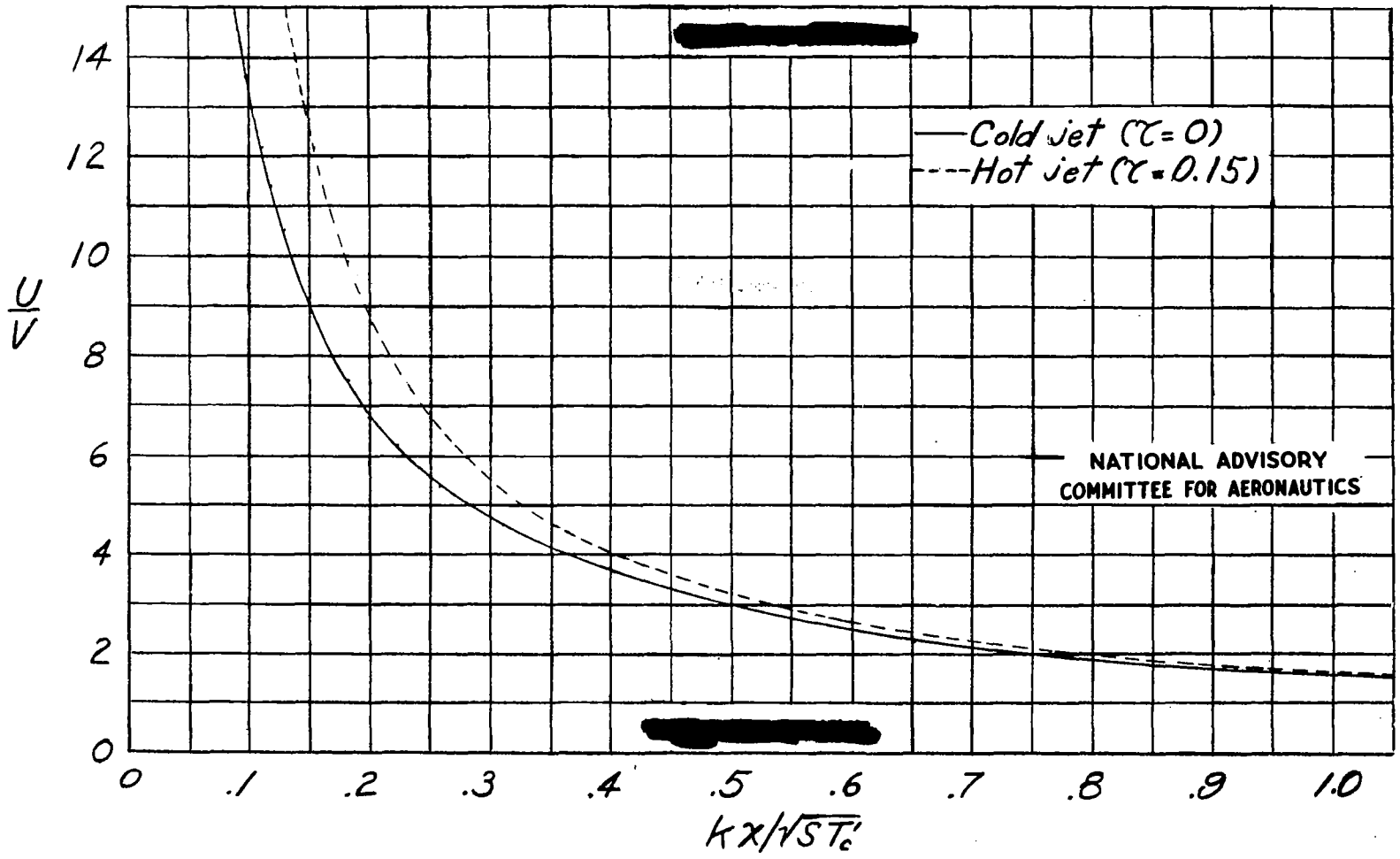

Figure 4.- Variation of the ratio $\frac{\text{Velocity on jet axis - Stream velocity}}{\text{Stream velocity}}$ with $kx/\sqrt{ST_c'}$.

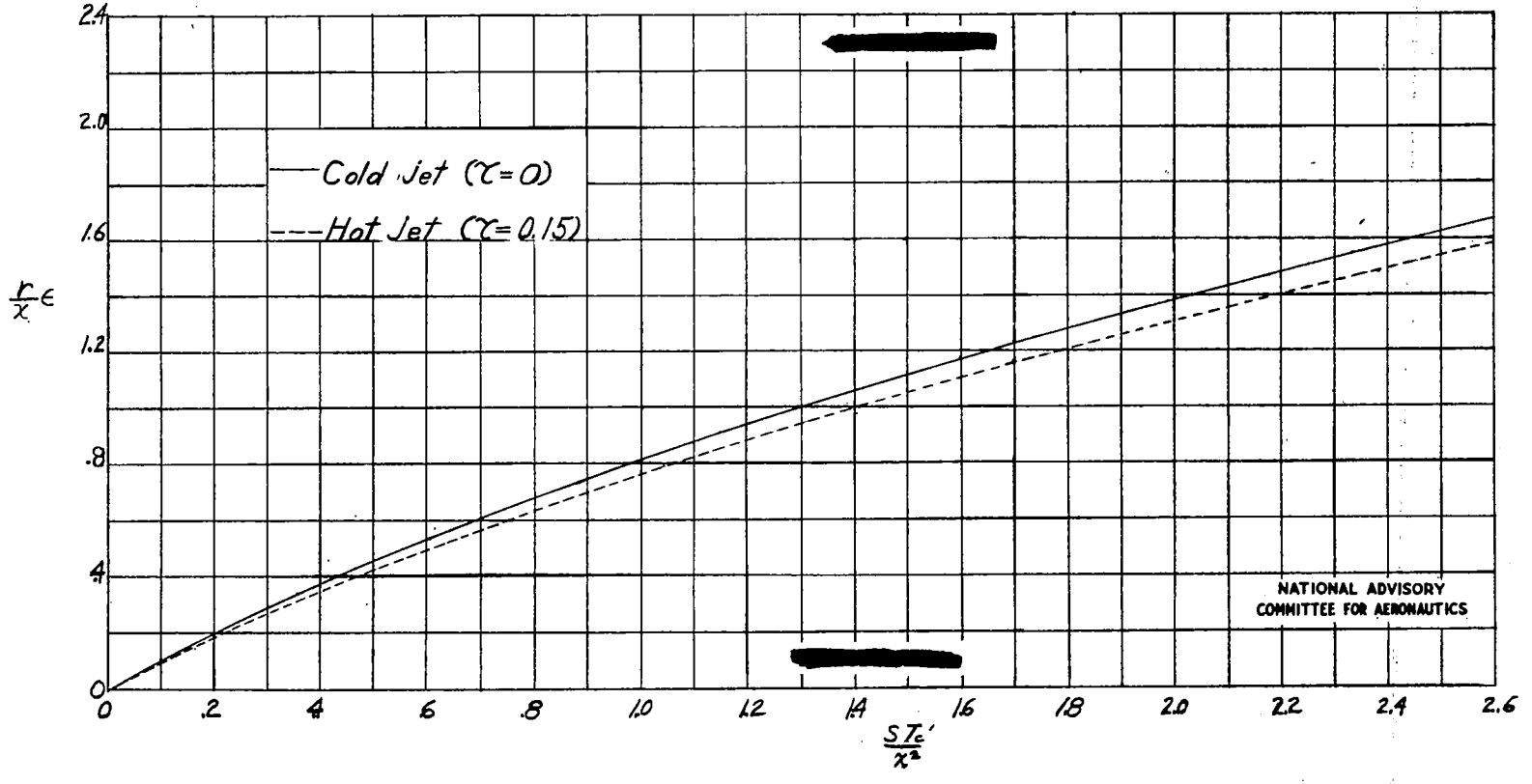

Figure 5.- Flow inclination outside a jet: variation of $\frac{r}{x}\epsilon$ with ST_c'/x^2. ϵ in degrees.

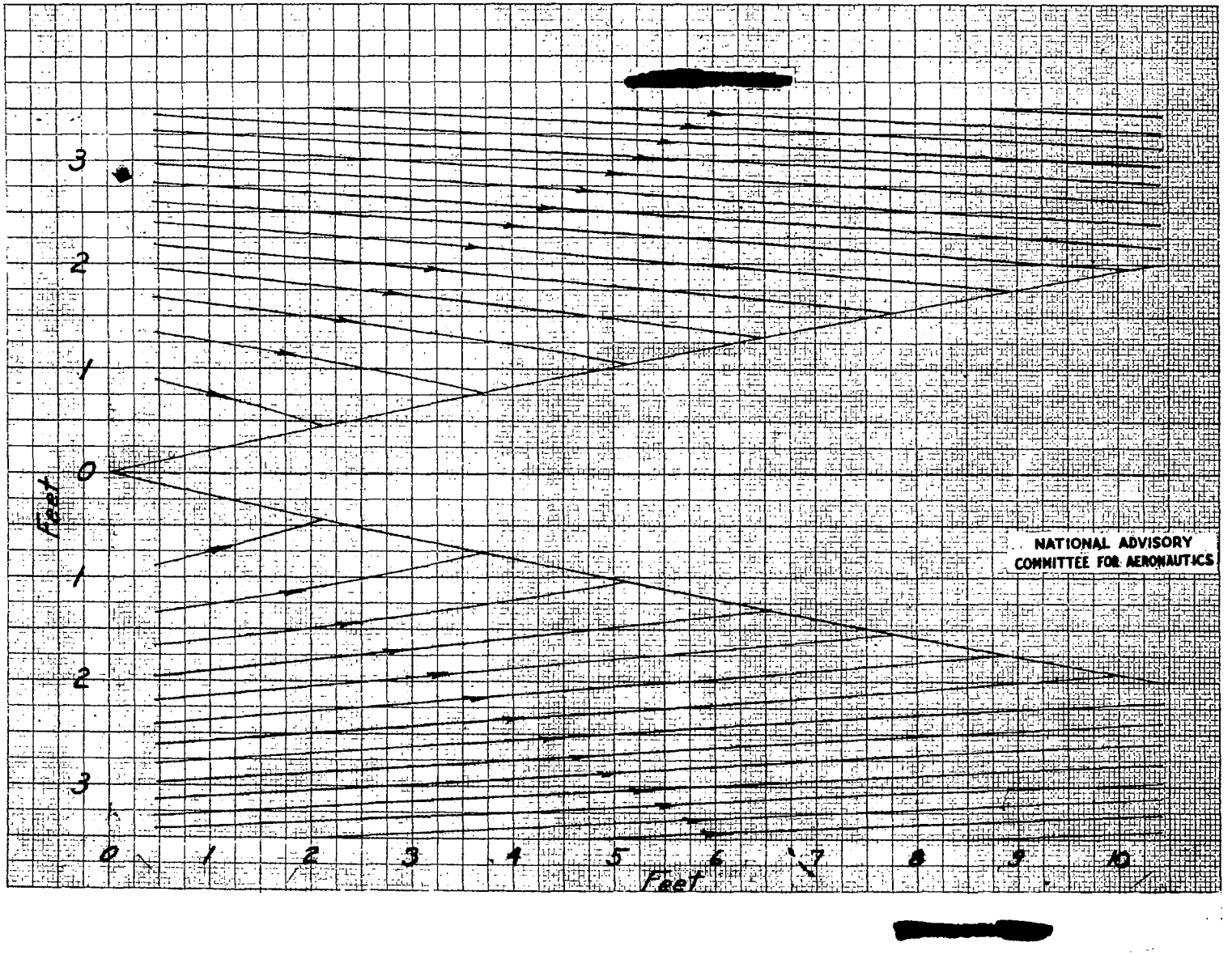

Figure 6.- Representative streamline pattern outside a jet of a jet-propelled airplane in flight.

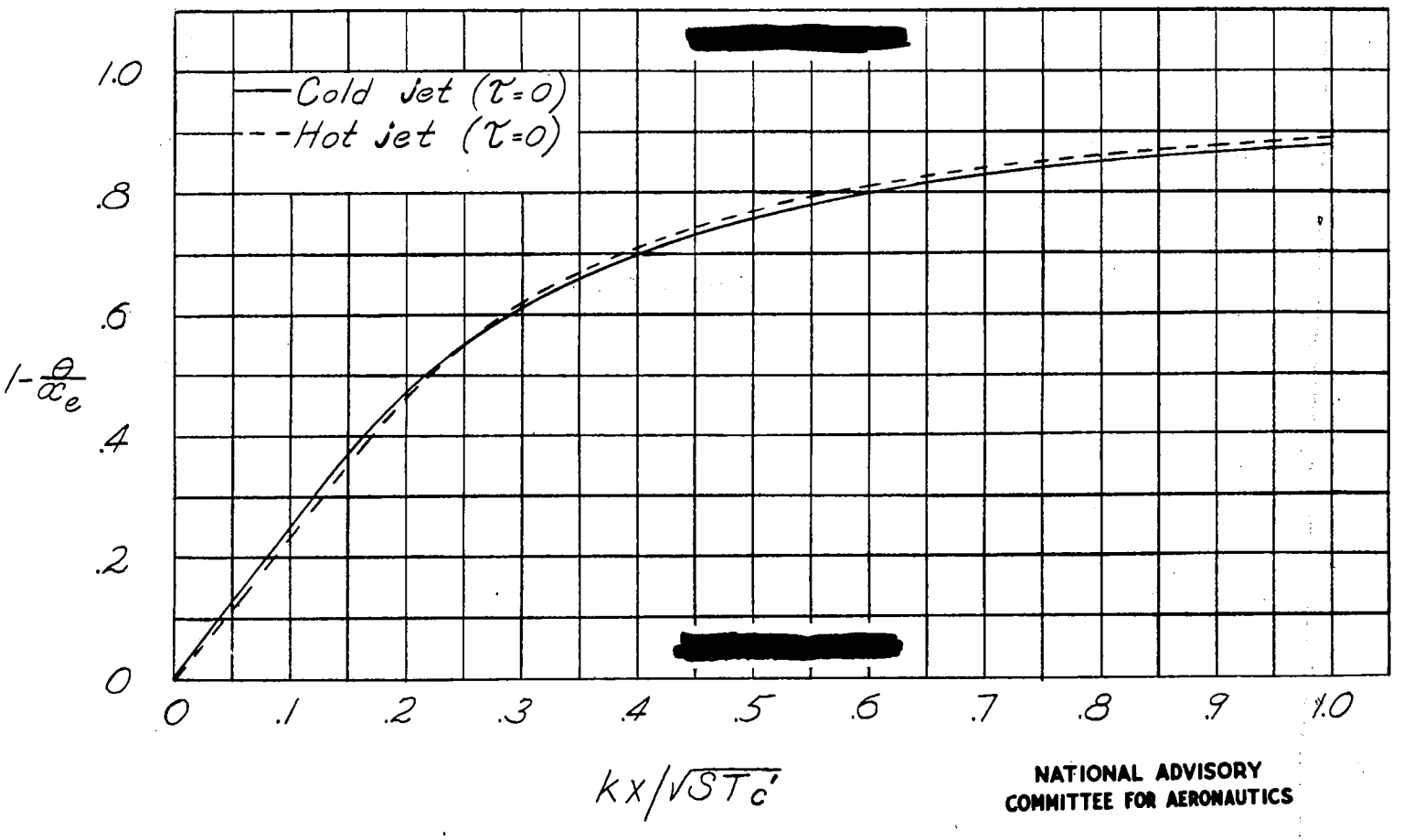

Figure 7.- Angular deviation of jet due to angle of attack: variation of $1 - \frac{\theta}{\alpha_e}$ with $kx/\sqrt{ST_c'}$.

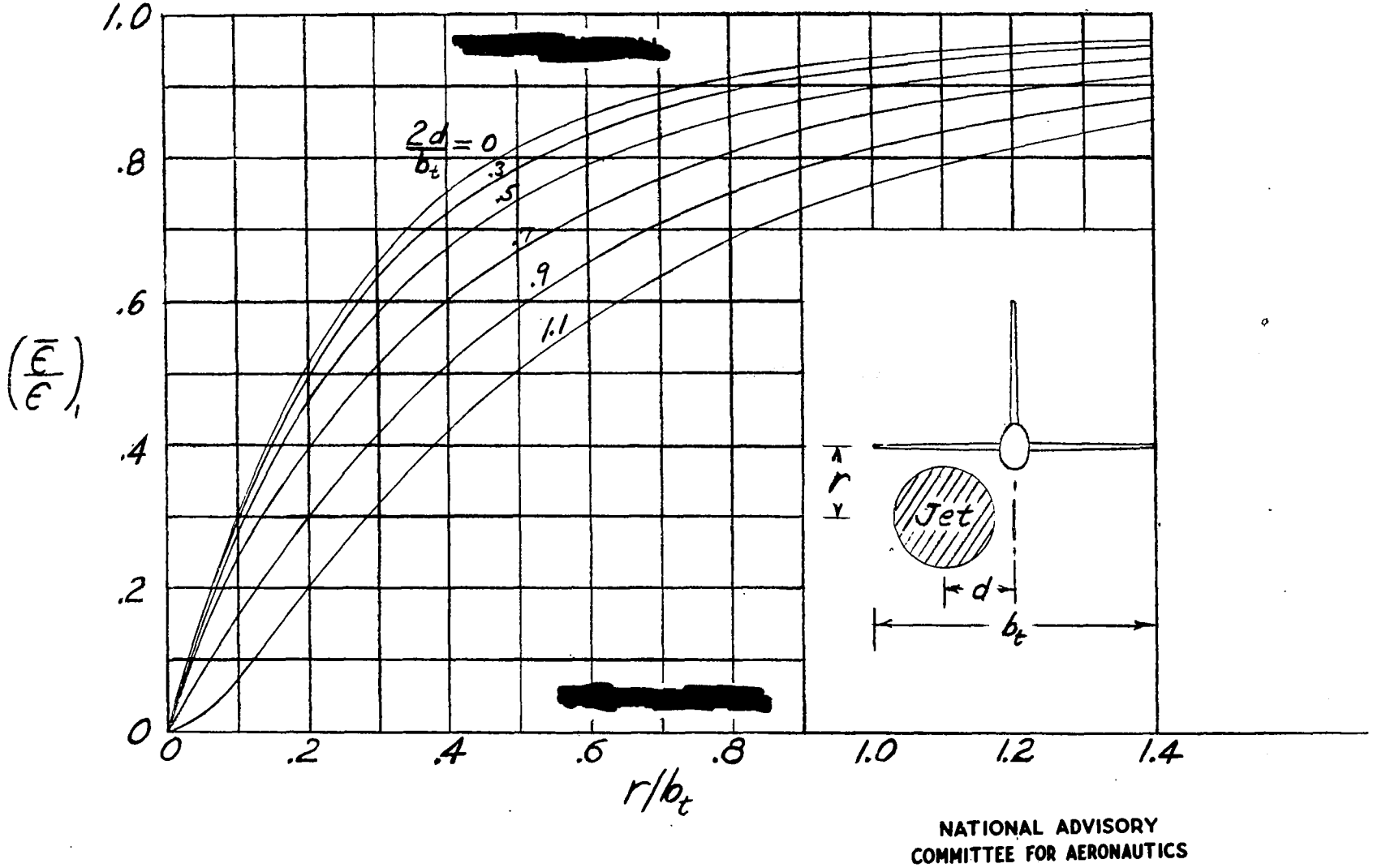

Figure 8.- Ratio of the effective mean downwash $\bar{\epsilon}$ induced by the jet over the tail plane to the flow inclination ϵ induced at a radius r.

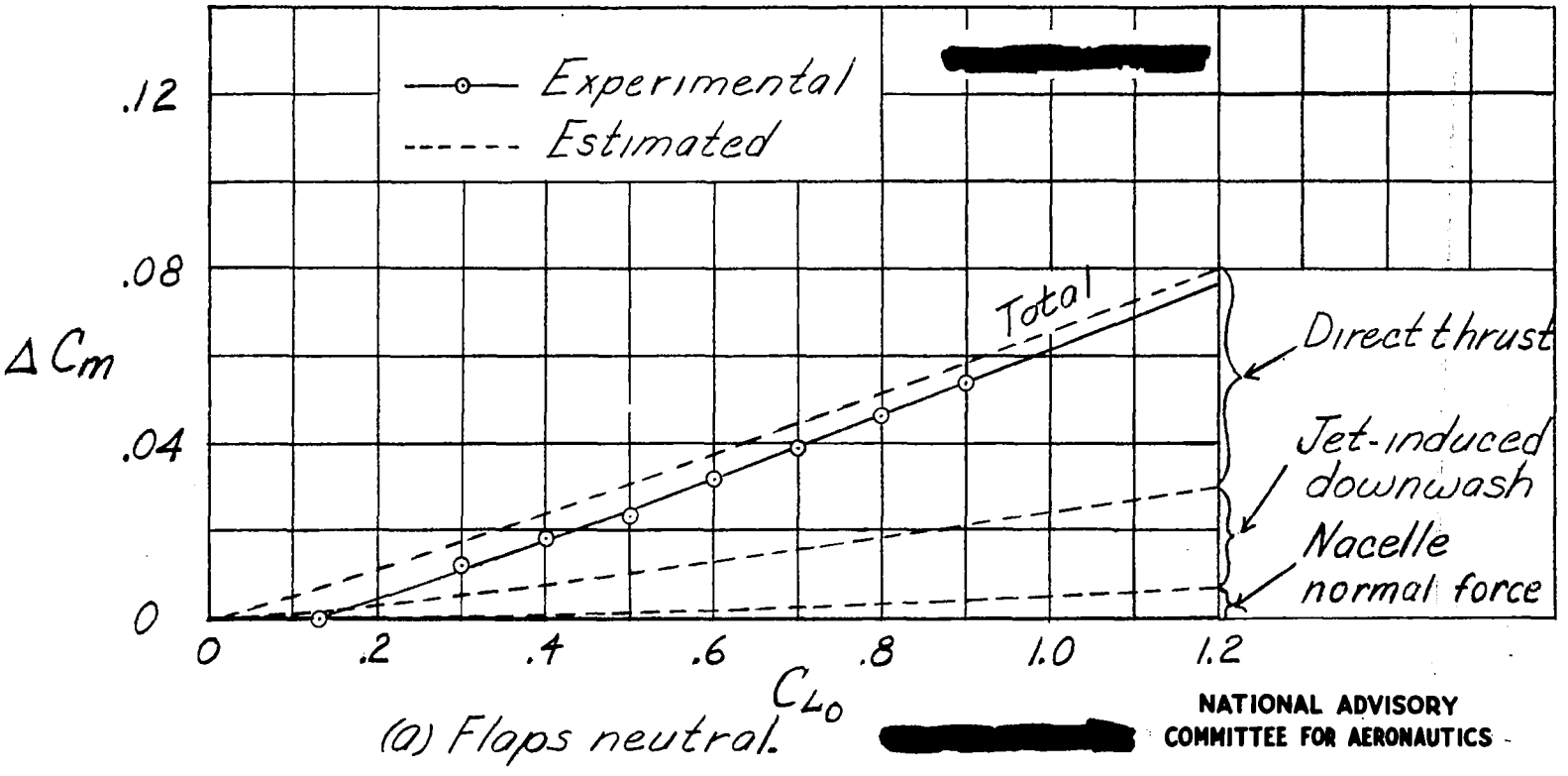

Figure 9.- Experimental and estimated increments of pitching-moment coefficient due to jet operation. Twin-jet fighter-type airplane, rated power at sea level. Experimental data from unpublished full-scale wind-tunnel tests.

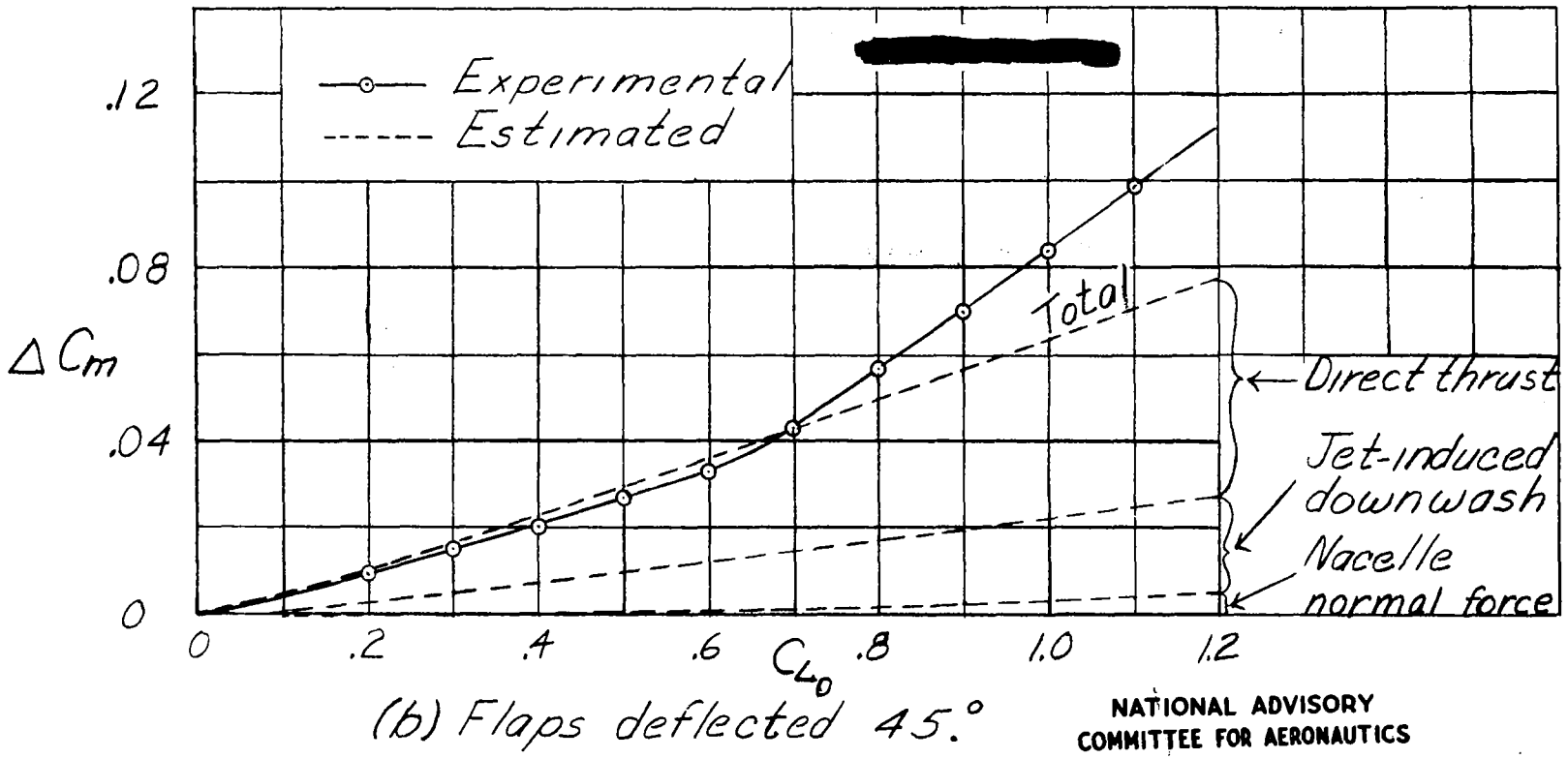

Figure 9.- Concluded.

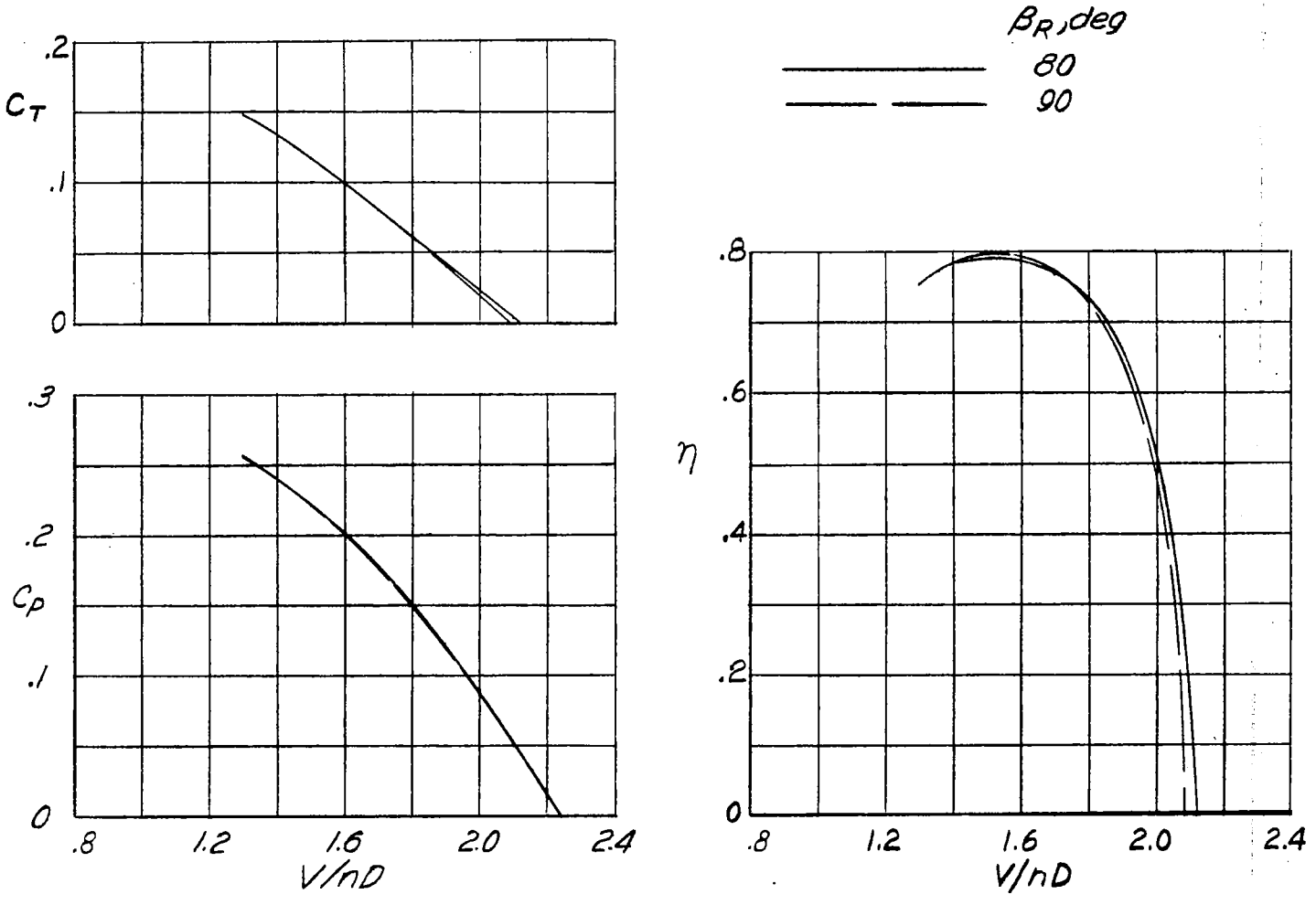

(c) Pusher propeller; $\beta_F = 40^\circ$; rear propeller locked.

Figure 5.- Continued.

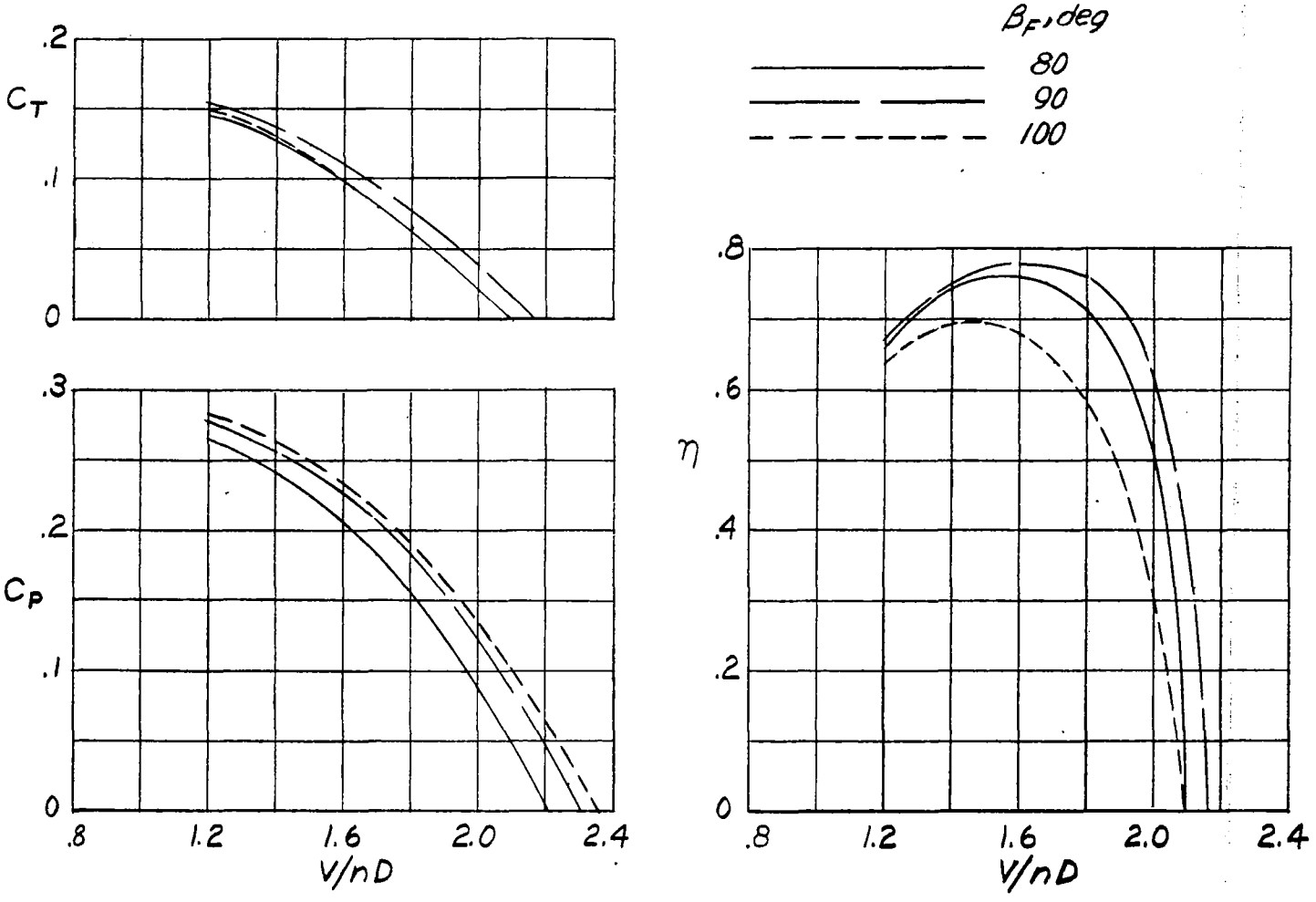

(d) Pusher propeller; $\beta_R = 40°$; front propeller locked.

Figure 5.- Concluded.

NATIONAL ADVISORY
COMMITTEE FOR AERONAUTICS

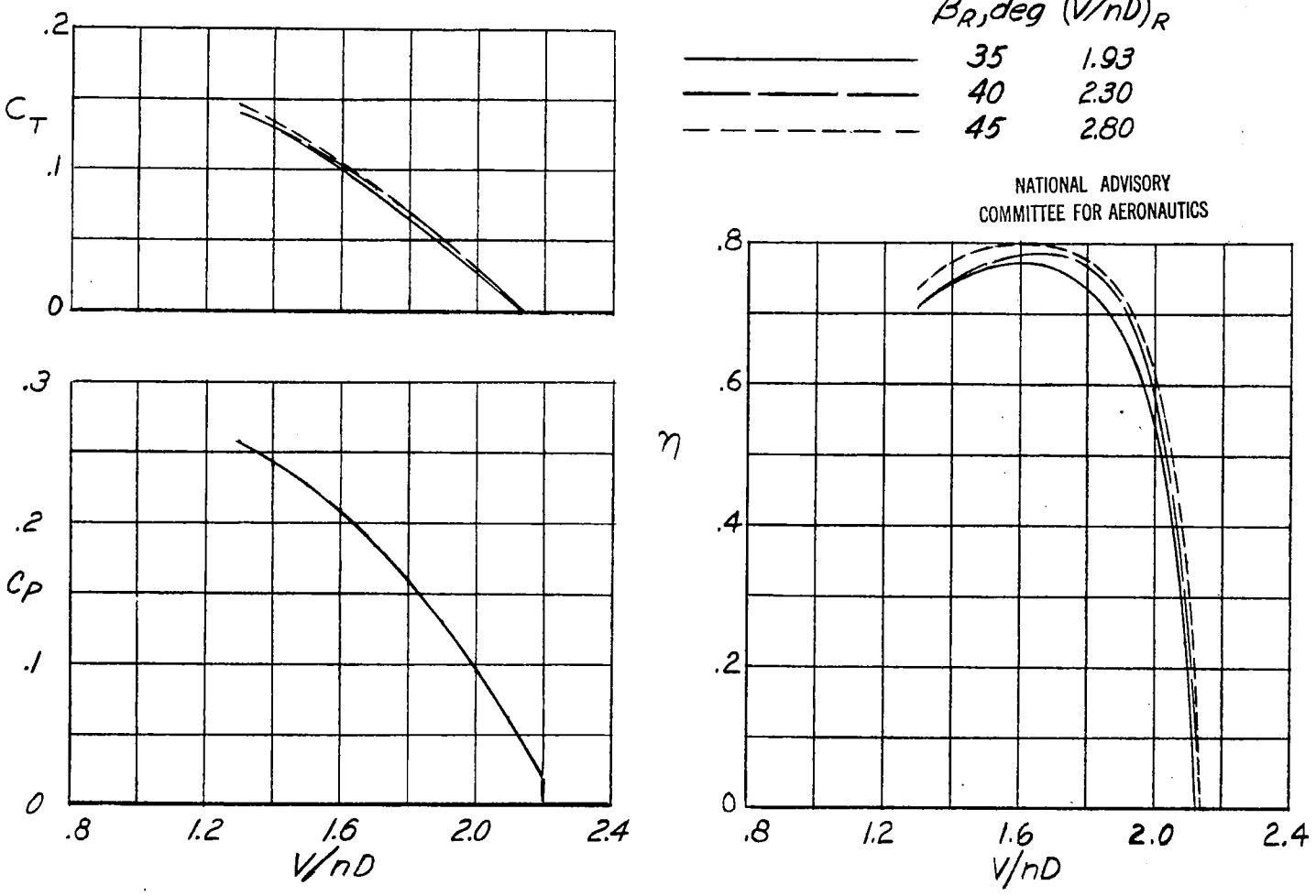

(a) Tractor propeller; $\beta_F = 40°$; rear propeller windmilling.

Figure 6.- Aerodynamic characteristics of the three-blade propeller operating in conjunction with the windmilling propeller.

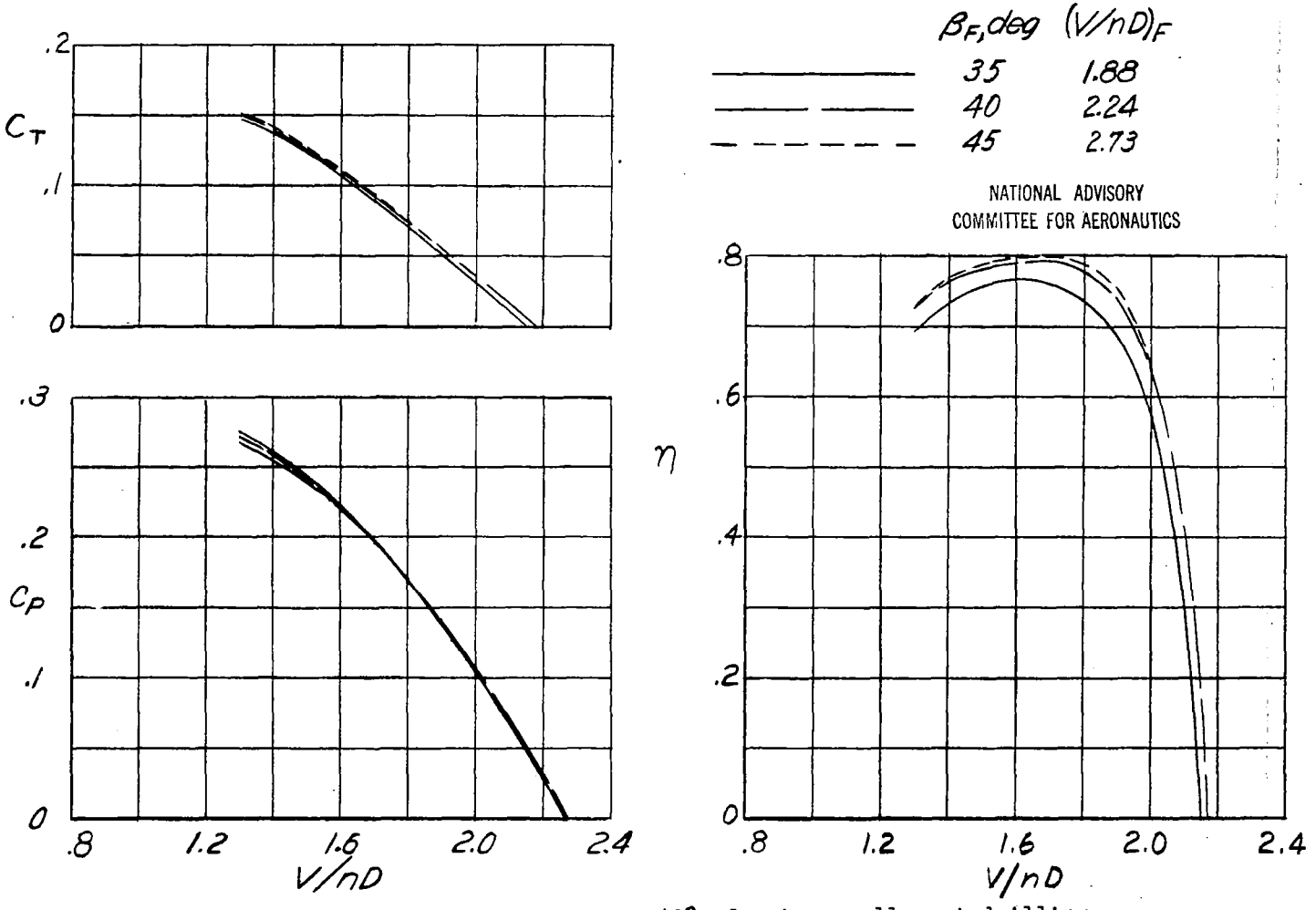

(b) Tractor propeller; $\beta_R = 40^\circ$; front propeller windmilling.

Figure 6.- Continued.

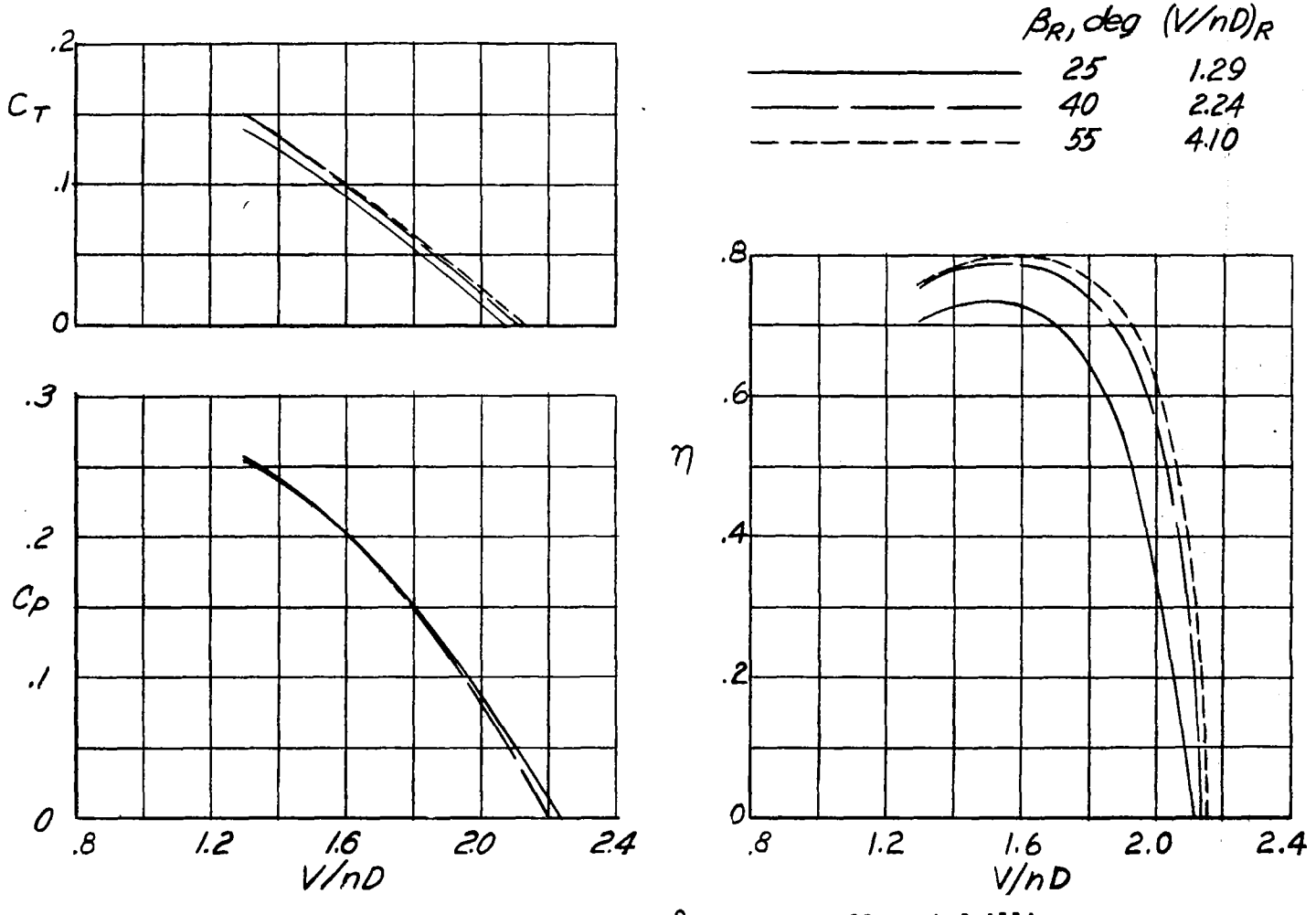

(c) Pusher propeller; $\beta_F = 40^\circ$; rear propeller windmilling.

Figure 6.- Continued.

NATIONAL ADVISORY
COMMITTEE FOR AERONAUTICS

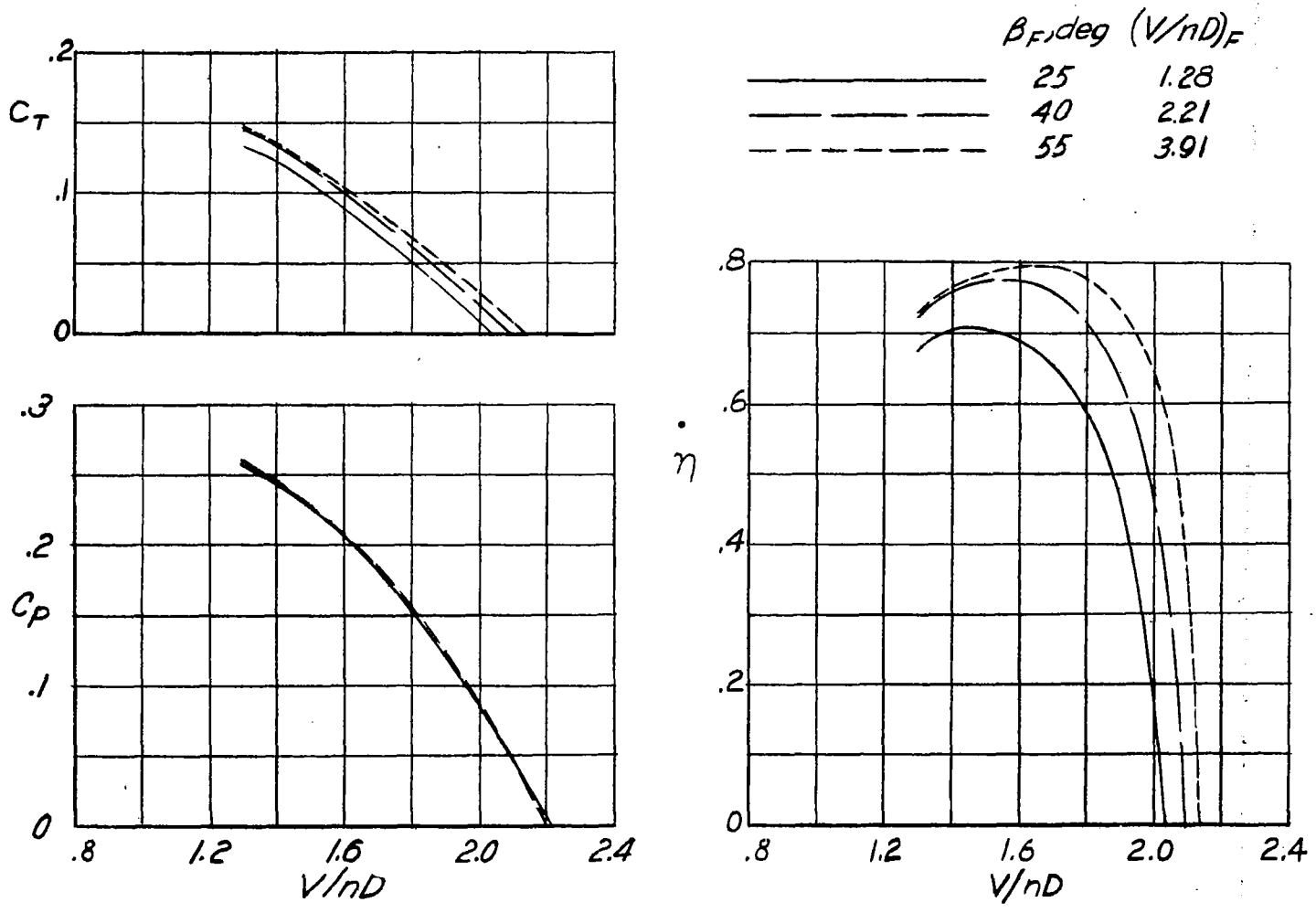

(d) Pusher propeller; $\beta_R = 40^\circ$; front propeller windmilling.

Figure 6.- Concluded.

NATIONAL ADVISORY
COMMITTEE FOR AERONAUTICS

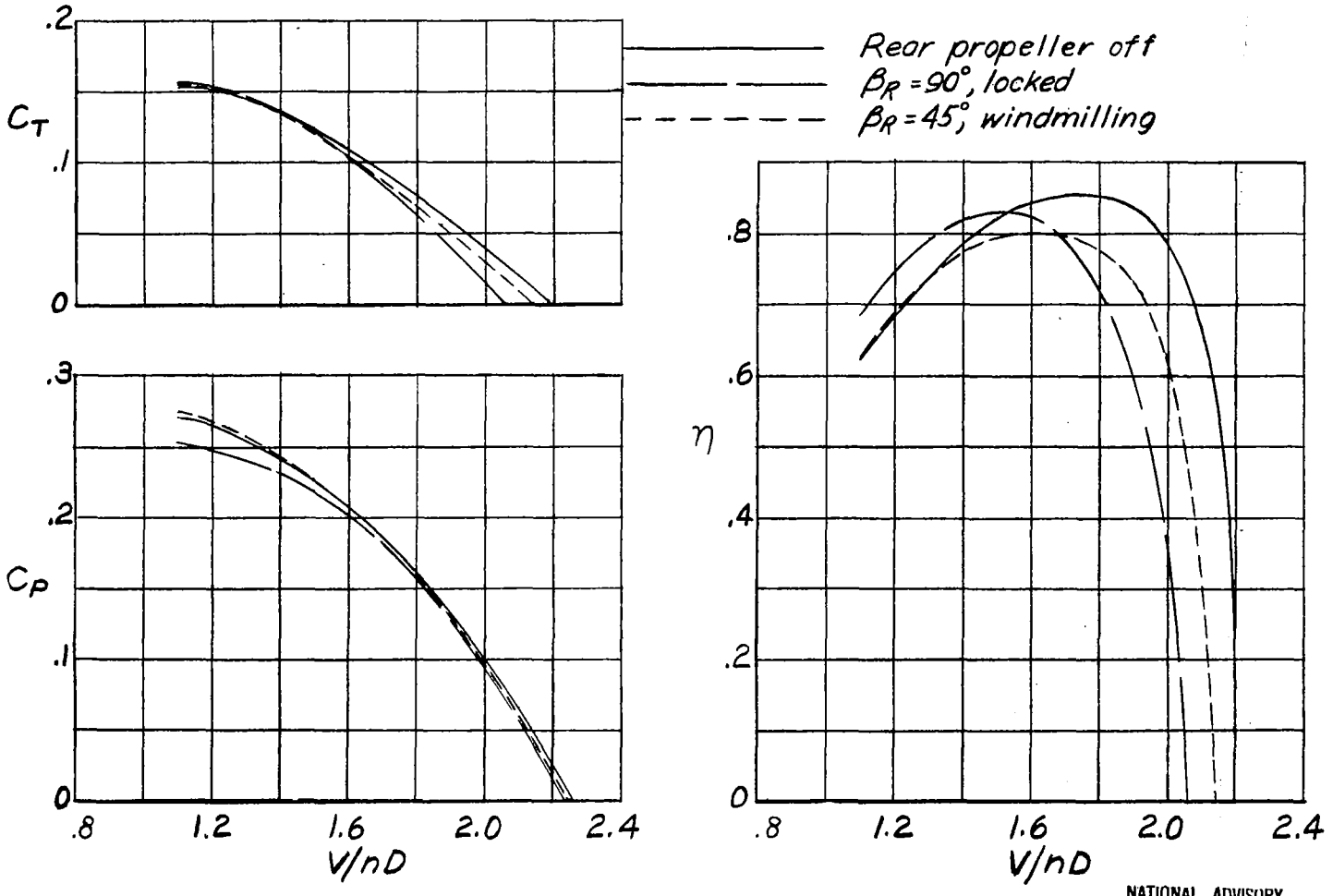

(a) Tractor propeller; β_F = 40°; front propeller driven.

NATIONAL ADVISORY COMMITTEE FOR AERONAUTICS

Figure 7.- Comparison of the aerodynamic characteristics of the three-blade propeller operating alone and in optimum combination with the locked or windmilling propeller.

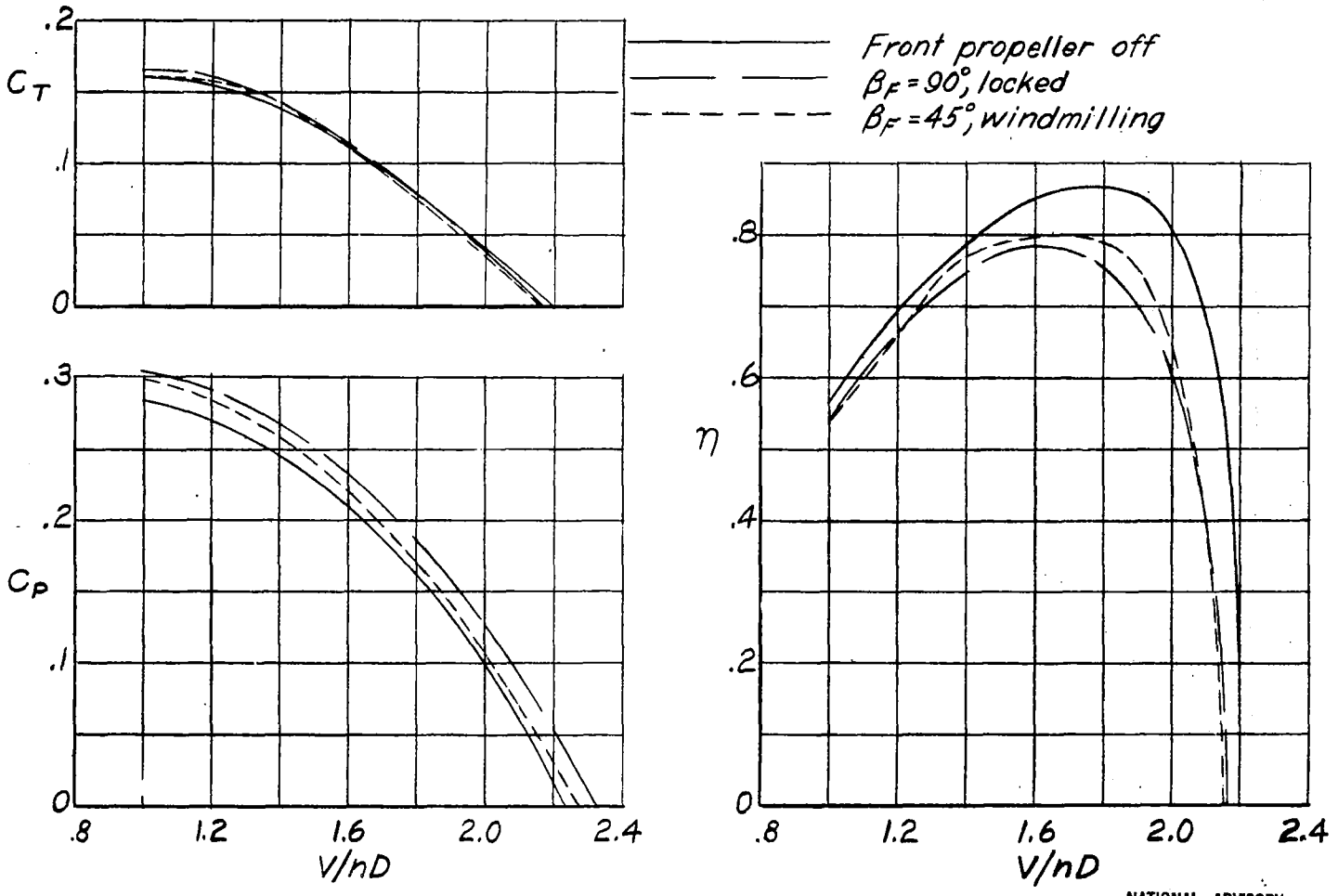

(b) Tractor propeller; $\beta_R = 40°$; rear propeller driven.

NATIONAL ADVISORY COMMITTEE FOR AERONAUTICS

Figure 7.- Continued.

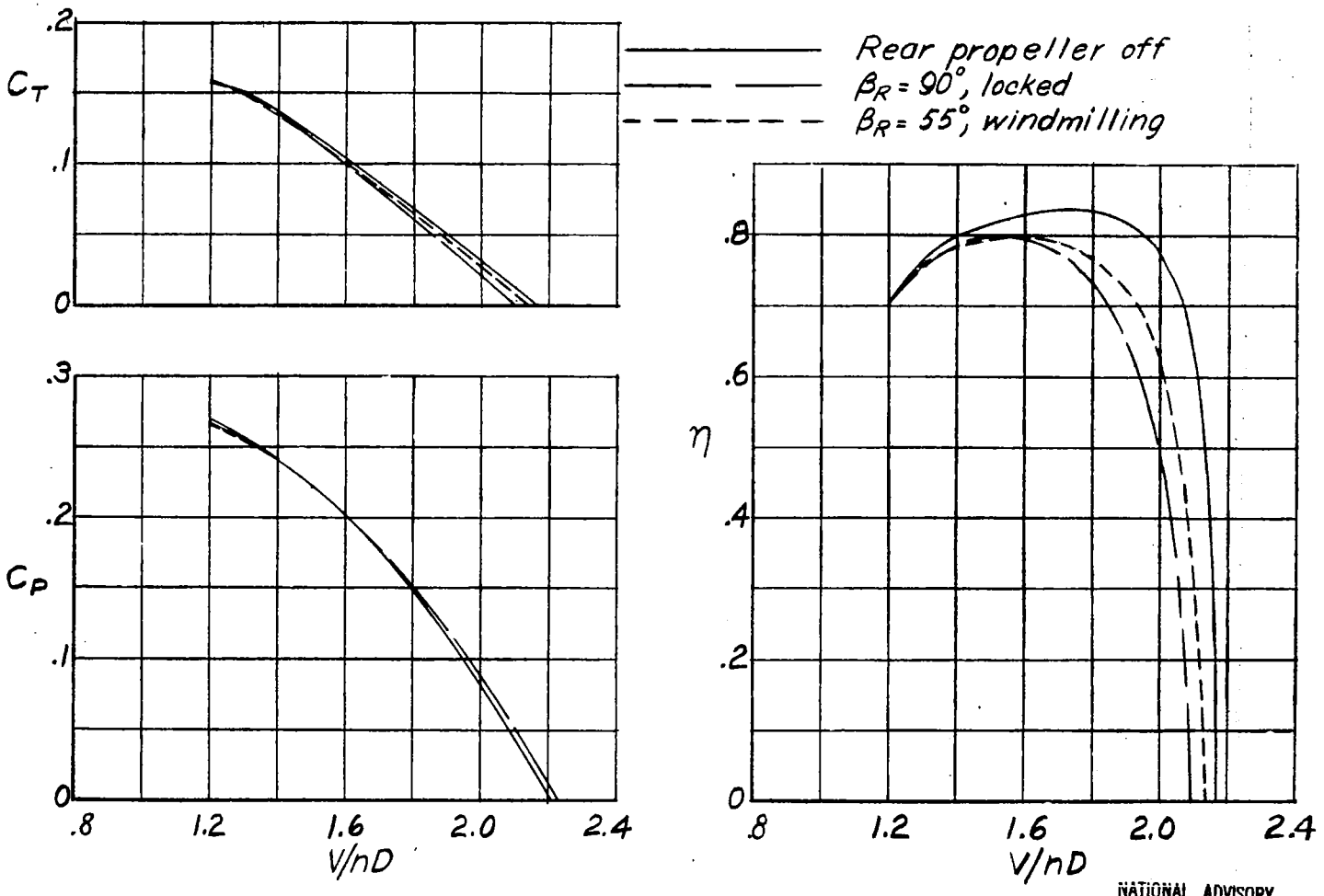

(c) Pusher propeller; $\beta_F = 40°$; front propeller driven.

NATIONAL ADVISORY COMMITTEE FOR AERONAUTICS

Figure 7.- Continued.

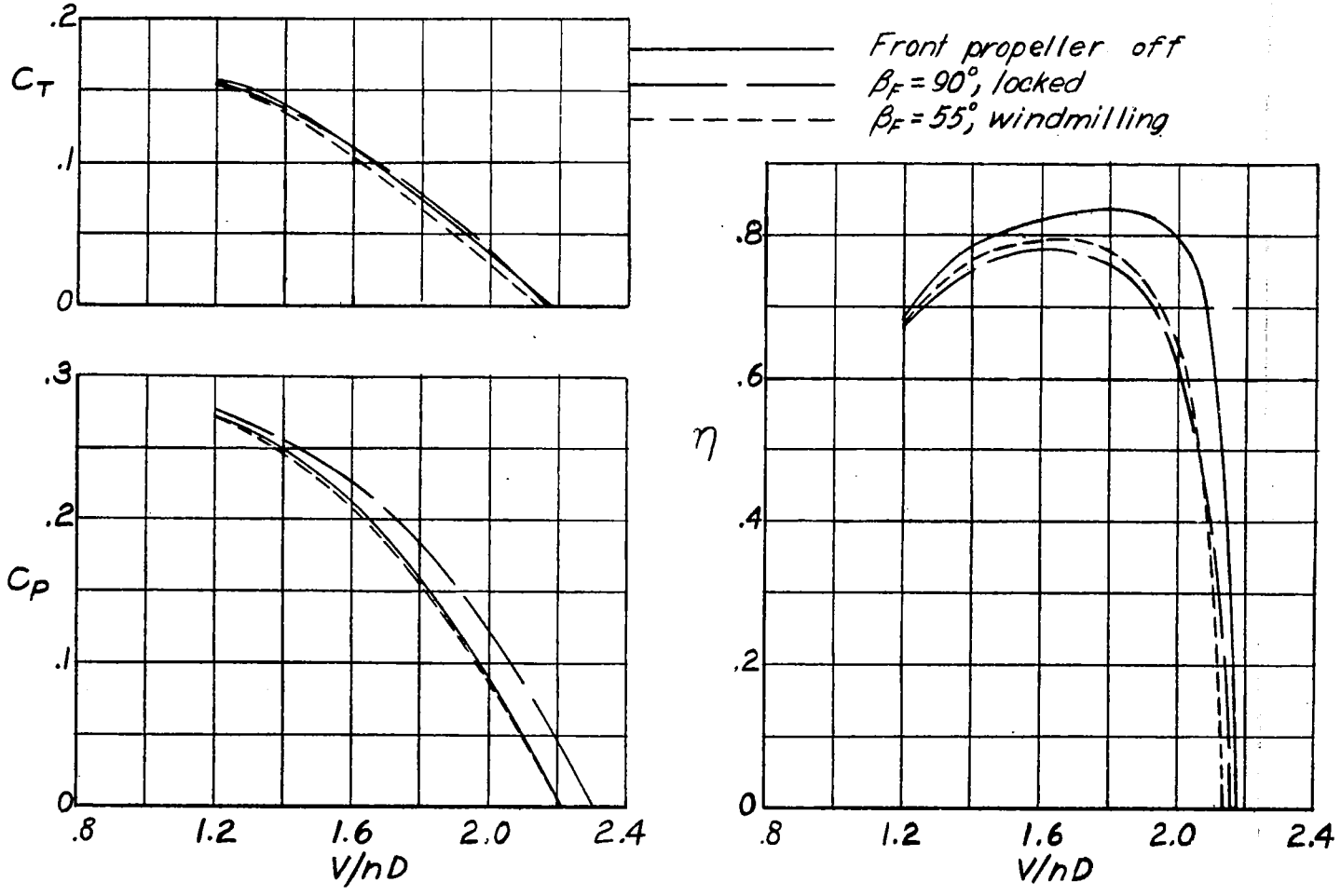

(d) Pusher propeller; $\beta_R = 40°$; rear propeller driven.

Figure 7.- Concluded.

NATIONAL ADVISORY
COMMITTEE FOR AERONAUTICS